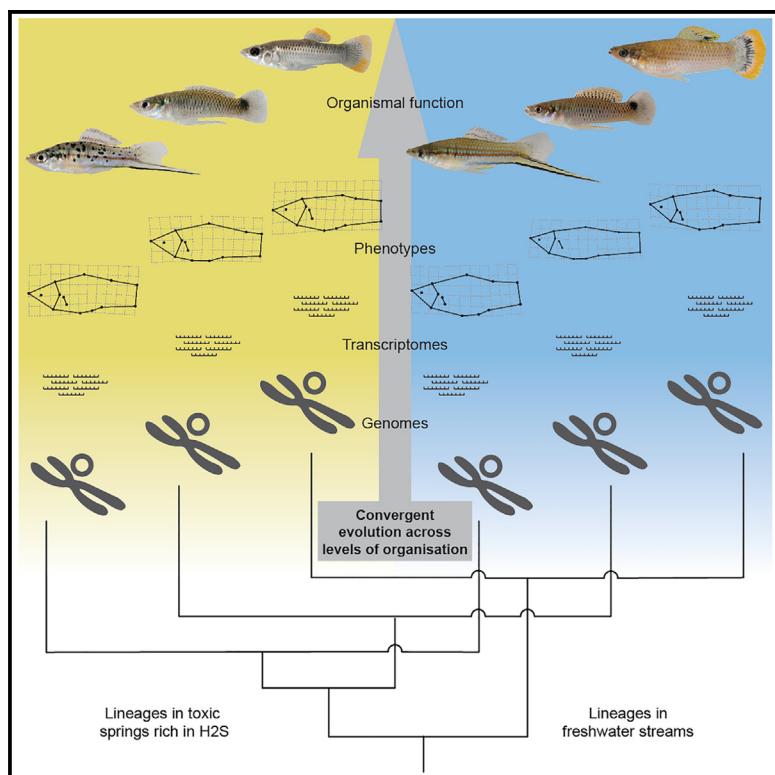


Integrative analyses of convergent adaptation in sympatric extremophile fishes

Graphical abstract



Authors

Ryan Greenway, Rishi De-Kayne,
Anthony P. Brown, ...,
Lenin Arias-Rodriguez,
Joanna L. Kelley, Michael Tobler

Correspondence

jokelley@ucsc.edu (J.L.K.),
tobler@umsl.edu (M.T.)

In brief

Convergent evolution is rarely studied in disparate but sympatric lineages. Greenway et al. study extremophile fishes and find that exposure to the same source of divergent selection results in variable degrees of convergence across different levels of biological organization.

Highlights

- A novel system with three lineages evolving along the same ecological gradient
- Selection from toxic hydrogen sulfide drives trait divergence at small spatial scales
- Convergence is evident in morphology, physiology, and the mitochondrial genome
- Genomic divergence is characterized by non-convergent, lineage-specific changes



Article

Integrative analyses of convergent adaptation in sympatric extremophile fishes

Ryan Greenway,¹ Rishi De-Kayne,² Anthony P. Brown,^{3,8} Henry Camarillo,^{1,9} Cassandra Delich,¹ Kerry L. McGowan,³ Joel Nelson,³ Lenin Arias-Rodriguez,⁴ Joanna L. Kelley,^{2,*} and Michael Tobler^{5,6,7,10,*}

¹Kansas State University, Division of Biology, 116 Ackert Hall, Manhattan, KS 66506, USA

²University of California Santa Cruz, Department of Ecology and Evolutionary Biology, 1156 High Street, Santa Cruz, CA 95064, USA

³Washington State University, School of Biological Sciences, 301 Abelson Hall, Pullman, WA 644236, USA

⁴Universidad Juárez Autónoma de Tabasco, División Académica de Ciencias Biológicas, Carretera Villahermosa-Cárdenas Km. 0.5 S/N, Entronque a Bosques de Saloya, 86150 Villahermosa, Tabasco, Mexico

⁵University of Missouri, St. Louis, Department of Biology, 1 University Boulevard, St. Louis, MO 63121, USA

⁶University of Missouri, St. Louis, Whitney R. Harris World Ecology Center, 1 University Boulevard, St. Louis, MO 63121, USA

⁷Saint Louis Zoo, WildCare Institute, 1 Government Drive, St. Louis, MO 63110, USA

⁸Present address: University of California, Davis, California National Primate Research Center, 1 Shields Avenue, Davis, CA 95616, USA

⁹Present address: Yale University, Department of Ecology and Evolutionary Biology, 165 Prospect Street, New Haven, CT 06520, USA

¹⁰Lead contact

*Correspondence: jokelley@ucsc.edu (J.L.K.), tobler@umsl.edu (M.T.)

<https://doi.org/10.1016/j.cub.2024.09.027>

SUMMARY

The evolution of independent lineages along replicated environmental transitions frequently results in convergent adaptation, yet the degree to which convergence is present across multiple levels of biological organization is often unclear. Additionally, inherent biases associated with shared ancestry and variation in selective regimes across geographic replicates often pose challenges for confidently identifying patterns of convergence. We investigated a system in which three species of poeciliid fishes sympatrically occur in a toxic spring rich in hydrogen sulfide (H_2S) and an adjacent nonsulfidic stream to examine patterns of adaptive evolution across levels of biological organization. We found convergence in morphological and physiological traits and genome-wide patterns of gene expression among all three species. In addition, there were shared signatures of selection on genes encoding H_2S toxicity targets in the mitochondrial genomes of each species. However, analyses of nuclear genomes revealed neither evidence for substantial genomic islands of divergence around genes involved in H_2S toxicity and detoxification nor substantial congruence of strongly differentiated regions across population pairs. These non-convergent, heterogeneous patterns of genomic divergence may indicate that sulfide tolerance is highly polygenic, with shared allele frequency shifts present at many loci with small effects along the genome. Alternatively, H_2S tolerance may involve substantial genetic redundancy, with non-convergent, lineage-specific variation at multiple loci along the genome underpinning similar changes in phenotypes and gene expression. Overall, we demonstrate variability in the extent of convergence across organizational levels and highlight the challenges of linking patterns of convergence across scales.

INTRODUCTION

Evolutionarily independent lineages often evolve similar solutions when facing similar ecological conditions. Although such patterns of convergence may provide evidence for the repeatability and predictability of evolution by natural selection,^{1–3} it can be challenging to determine the extent of convergence across levels of biological organization and, ultimately, whether convergent genomic shifts underpin convergence at other scales.⁴ Convergent evolution is frequently studied in closely related, but geographically disjunct, population pairs exposed to similar sources of divergent selection, providing spatially replicated instances of local adaptation within a clade.¹ Investigations into convergent evolution in

such systems have provided valuable insights across a variety of animal and plant systems by highlighting instances of evolutionary convergence at the level of single genes^{5,6} and more polygenic signals of convergence.^{7,8} However, studies that focus on closely related lineages likely bias our understanding of general patterns of convergence because shared evolutionary responses may be the result of selection on standing genetic variation and constraints associated with shared genomic architecture.^{5,9,10} Similarly, the focus on geographically disjunct populations exposed to seemingly similar selective regimes has the potential to ignore the effects of unquantified environmental variation, which often leads to idiosyncratic evolutionary responses.^{11,12} Studying distantly related taxa that are experiencing a shared selective



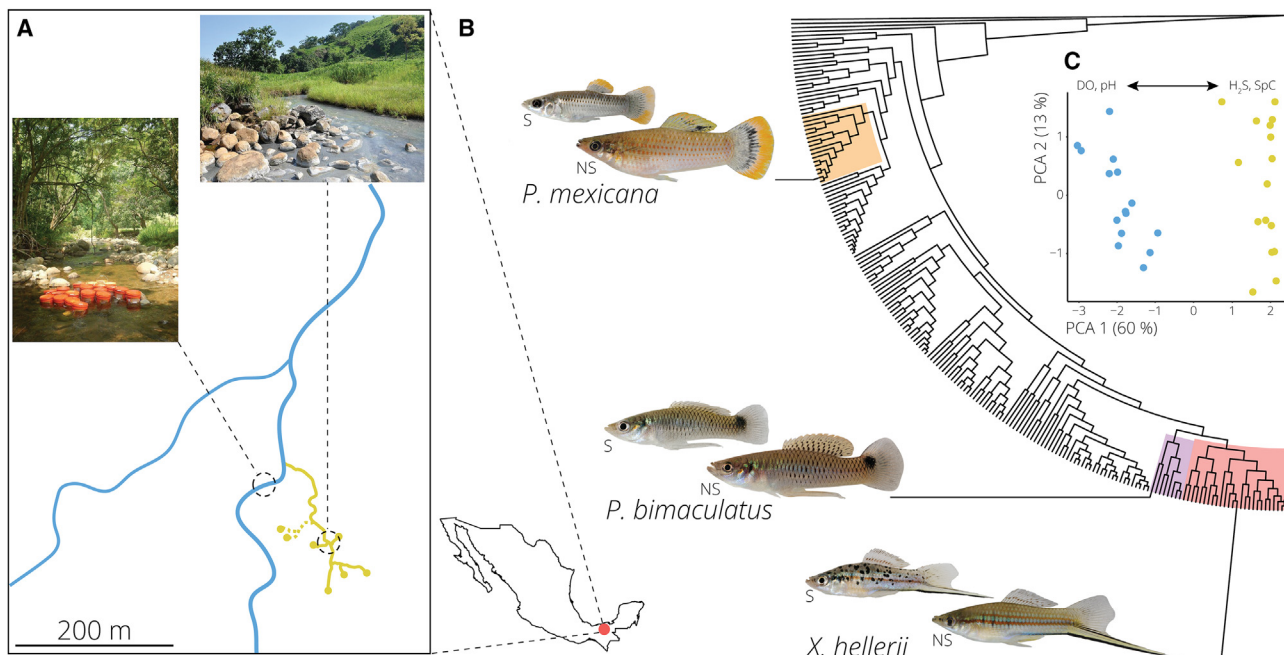


Figure 1. Sympatric populations of three highly divergent poeciliid lineages co-occur in a sulfide spring and adjacent nonsulfidic stream in southern Mexico

(A) Map of the study site, where yellow points indicate the H₂S spring heads of the La Gloria spring system, while yellow lines indicate H₂S-rich stream segments. Blue lines indicate the adjacent nonsulfidic stream system, Arroyo Caracol. Inset photos depict representative habitats within the two streams (top: La Gloria, sulfidic; left: Arroyo Caracol, nonsulfidic).

(B) Phylogeny of the family Poeciliidae highlighting the three focal genera: *Poecilia* (orange), *Pseudoxiphophorus* (purple), and *Xiphophorus* (red). Each species' position within its genus is denoted by the extended branch leading to representative photographs of a sulfidic (S; top) and nonsulfidic (NS; bottom) male of each species. Note that the most basal split in the phylogeny is dated at 53.4–56.5 million years, and the most recent common ancestor of the three focal genera is dated ~40 million years.¹⁸

(C) Nonsulfidic and sulfidic habitats differed significantly in physical and chemical water parameters. Principal-component analysis indicated that sites within the La Gloria spring complex (yellow) and Arroyo Caracol (blue) separated along the primary axis of variation, with nonsulfidic sites exhibiting higher dissolved oxygen (DO) concentrations and pH and sulfidic sites exhibiting higher H₂S concentrations and specific conductivities (SpC).

environment in sympatry eliminates these confounding influences, providing the opportunity to investigate convergence in adaptive strategies and determine the predictability and repeatability of evolution.^{13–15}

We took advantage of a unique system to explore shared patterns of adaptive evolution among three sympatric lineages of live-bearing fishes (Poeciliidae). In Mexico, populations of *Poecilia mexicana*, *Pseudoxiphophorus bimaculatus*, and *Xiphophorus hellerii* coexist both within the La Gloria sulfide spring complex, which is characterized by high concentrations of naturally occurring hydrogen sulfide (H₂S), and in adjacent nonsulfidic streams (Figures 1A and 1B). The presence and absence of H₂S creates strong divergent selection across habitat types because of its toxic properties. H₂S binds to cytochrome c oxidase (COX) of the electron transport chain and interrupts oxidative phosphorylation (OxPhos) in mitochondria, ultimately stopping aerobic ATP production necessary for the maintenance of cellular function.^{16,17} At the molecular level, the clear biochemical and physiological consequences of H₂S predict adaptive modification of genes associated with OxPhos and enzymatic H₂S detoxification, which is mediated by the mitochondrial sulfide:quinone oxidoreductase (SQR) pathway.¹⁶ Besides the presence and absence of H₂S, the two aquatic habitats differ in other physical and chemical attributes, with sulfide spring habitats having lower

dissolved oxygen concentrations and pH but higher specific conductivity (Figure 1C).

The La Gloria system is particularly interesting because it allows for the juxtaposition of evolutionary responses to H₂S in distantly related species that occur in sympatry with evolutionary responses previously documented in geographically disparate populations of sulfide spring fishes within the family Poeciliidae.¹⁹ Throughout the Americas, highly endemic poeciliids locally adapted to sulfide springs have evolved from ancestral populations in adjacent freshwater habitats.^{19–21} Evolutionary responses to the toxic conditions have primarily been studied in geographically replicated populations of *Poecilia mexicana*, which exhibit convergence in morphology, physiology, life histories, gene expression, and the establishment of reproductive isolation as a byproduct of adaptation via ecological speciation.¹⁹ Although some convergence appears to result from *de novo* modification of the same genes or biochemical pathways (e.g., in OxPhos), there is also evidence for selection on standing genetic variation (e.g., in the SQR pathway).^{22–28} As in other systems, the focus on convergence across geographically replicated lineages within *P. mexicana* may have biased the interpretation of the repeatability and predictability of adaptive evolution in sulfide springs. Indeed, a recent broad-scale study of adaptation to sulfide springs across the Poeciliidae found evidence for

convergence in gene expression profiles of ten evolutionarily independent sulfide spring lineages, but only limited evidence for repeatable patterns of molecular evolution outside of a few mitochondrial encoded OxPhos genes.²⁶ The degree to which this breakdown of molecular convergence at a broader phylogenetic scale is related to differences in the selective regimes among geographically disparate sulfide springs or attributable to lineage-specific evolutionary solutions to a shared source of selection remains unresolved.

In this study, we aimed to identify signatures of convergence associated with the adaptation of three independent lineages to the same H₂S-rich spring. This approach helped reduce the confounding effects of shared ancestral standing genetic variation and allowed us to stringently test for shared adaptive responses across biological levels of organization in different species. Our results also provided the opportunity to identify possible links between different aspects of convergence across scales, including whether convergence in morphology and gene expression is explicitly underpinned by convergent genomic variation. To address this overarching hypothesis, we (1) identified signatures of convergent evolution in phenotypic traits that have previously been associated with adaptation to sulfide spring environments (body shape, H₂S tolerance, and gene expression), (2) established evidence for local adaptation between sulfidic and nonsulfidic populations of each species, and (3) identified convergent patterns of genomic differentiation among population pairs in sulfidic and nonsulfidic habitats. Overall, we found evidence for convergence in adaptation across multiple levels of organization, but convergence at the genomic level was limited and, outside of the mitochondrial genome, not associated with genomic regions predicted to respond to selection from H₂S.

RESULTS

Phenotypic variation among habitats

Mechanisms of adaptation to H₂S-rich environments have been studied extensively in poeciliid fishes, including the biochemical and physiological modifications that directly mitigate H₂S toxicity²⁶ and modifications of other traits that are shaped by sources of selection and that are correlated with the presence of H₂S, including hypoxia, increased salinity, changes in trophic resource use, competition, and predation.^{19,29} We quantified variation of natural populations in three complex traits that typically show adaptive divergence upon sulfide spring colonization: body shape, H₂S tolerance, and gene expression. We found that sulfide spring populations of all three focal species exhibit convergent patterns of trait divergence from adjacent nonsulfidic populations in response to colonization of sulfide springs.

Geometric morphometric analyses of wild-caught, adult fish revealed that body shape significantly differed between sulfidic and nonsulfidic populations of all three lineages (Procrustes ANOVA; species \times habitat: $p < 0.001$, $Z = 7.565$, Table S1). Furthermore, there was a significant signal of morphological convergence across the sulfide spring populations of the three species (habitat: $p = 0.018$, $Z = 2.093$, Table S1). Investigation of thin-plate spline transformation grids visualizing shape differences for both the “species \times habitat” and “habitat” terms indicated that the shared aspects of variation in body shape

between sulfidic and nonsulfidic populations of each species involved divergence in head size, with fish from the sulfide spring exhibiting larger heads than those from the nonsulfidic habitat (Figure 2A).

Survival analyses indicated that wild-caught, adult fish from all three sulfide spring populations exhibited an increased ability to tolerate acute H₂S exposure relative to nonsulfidic populations (Figure 2B; Cox regression; habitat: $p = 0.034$, Figure S1). Although H₂S tolerance was clearly affected by habitat of origin, differences in tolerance between sulfidic and nonsulfidic populations also varied among the three species, with sulfidic *P. mexicana* having a higher H₂S tolerance than both nonsulfidic *Poecilia* and sulfidic populations of the other species (Figure S1). This observation matched microhabitat uses by the three species within the sulfide spring complex; *P. mexicana* was the only species inhabiting immediate spring outlets with the highest H₂S concentrations, and the other two species were more common in areas with more oxygen-rich water (Figure S2).

Analysis of gene expression in gill tissues from wild-caught sulfidic and nonsulfidic fish revealed a phylogenetic signal in gene expression variation, with individuals clustering by species and, secondarily, by habitat type (Figure 3A). There were many differentially expressed genes (negative binomial regression, false discovery rate [FDR] < 0.05) between the sulfidic and nonsulfidic populations of each species, representing 13.4% of all measured genes for *Pseudoxiphophorus*, 20.4% for *Poecilia*, and 20.9% for *Xiphophorus* (Figure 3B). Although most gene expression differences were species specific (Data S1), 245 genes (1.3% of all analyzed genes; 6.3%–9.8% of differentially expressed genes in each species) exhibited convergent expression changes across all species (153 upregulated, 92 downregulated; Figure 3B; Data S1), significantly more than predicted by chance (SuperExactTest³⁰: $p < 0.0001$). As predicted by the biochemical and physiological effects of H₂S, analysis of Gene Ontology (GO) IDs associated with differentially expressed genes revealed that shared upregulated genes were significantly enriched (FDR < 0.05) for associations with mitochondria and biological processes involved in H₂S toxicity and detoxification, including aerobic respiration and the electron transport chain (OxPhos), enzymatic H₂S detoxification, and the processing and transport of sulfur compounds (Data S2). Notably, we found consistent upregulation of genes associated with the primary target of H₂S toxicity (COX) and the primary H₂S detoxification pathway (SQR pathway; Figures 3C–3E). There was no evidence for significant enrichment of any GO terms in downregulated genes (Data S2).

Population structure

As phenotypic divergence between sulfidic and nonsulfidic populations of each species was measured using wild-caught fish, we cannot rule out the possibility that both adaptation and phenotypic plasticity contribute in some part to phenotypic responses to the colonization of the sulfidic habitat. However, because divergent selection on key ecological traits generally reduces gene flow between populations, local adaptation and phenotypic plasticity are predicted to have different population genomic signatures. When plasticity alone underpins phenotypic differentiation across environmental contrasts, we expect to see little genome-wide population structure, as gene flow between

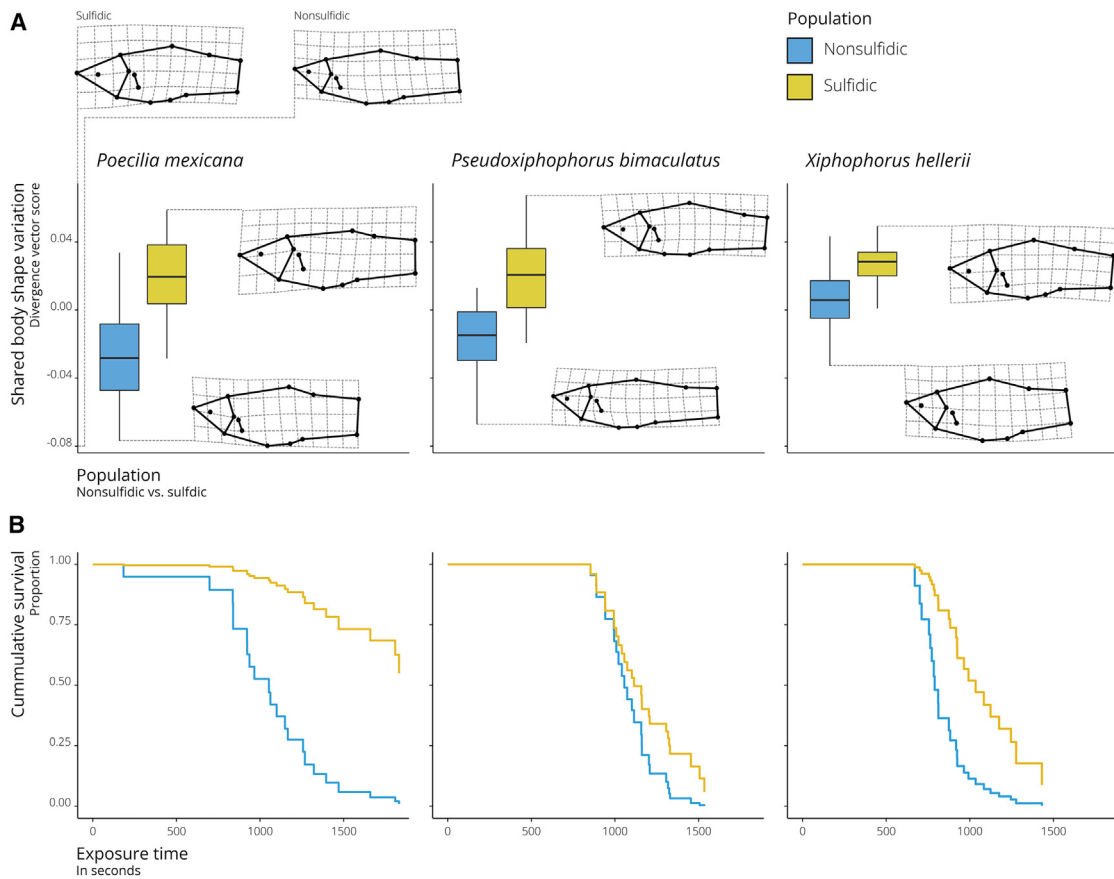


Figure 2. Phenotypic convergence in morphological and physiological traits of sympatric sulfidic populations

(A) Convergent morphological evolution among species between habitat types as indicated by boxplots of divergence vector scores. Body shape differentiation along a shared axis of divergence (habitat type) is depicted by the transformation grids on the top. Significant differences in body shape between populations of each species is depicted in insets (Table S1).
 (B) Convergence in H₂S tolerance among all populations from the sulfidic habitat. Cumulative survival in acute H₂S toxicity trials revealed significant differences between populations, which were most pronounced in *P. mexicana* (Figure S1). Differences among sulfidic lineages may be related to differential microhabitat use among species (Figure S2).

habitats prevents genomic differentiation from establishing. In contrast, where divergent selection has resulted in the establishment of barriers to gene flow, we expect to find lower rates of gene flow between populations and signals of population structure, even though the La Gloria sulfide spring complex is spatially restricted (~200 m in length), flows directly into the adjacent non-sulfidic stream (Figure 1A), and there are no physical barriers preventing fish movement between habitat types. Additionally, previous investigations into the signatures of gene expression associated with adaptation of *P. mexicana* to sulfide springs have provided evidence of heritable variation in gene expression,^{31,32} which highlights the potential for a component of adaptation to be underpinned by genomic variation rather than plasticity alone. To test for genetic signatures of local adaptation, we sampled 20 individuals per species in each habitat type and conducted population genomic analyses based on whole-genome resequencing (average sequence depth per individual: 3.8 ± 0.4 ; Table S2) to infer population structure between the sulfidic and nonsulfidic populations. Maximum-likelihood-based estimates of admixture proportions with two inferred clusters

($k = 2$) unambiguously clustered individuals by their habitat type of origin and only detected low levels of admixture between sulfidic and nonsulfidic populations within each species (Figure 4A), indicating a substantial reduction in gene flow between the two habitats. Principal-component analysis (PCA) and demographic models corroborated these results (Figures S3 and S4). Both structure analysis and PCA identified two *P. mexicana* individuals that appear to be early-generation hybrids (F1 and a possible F2 backcross), while all other individuals of all species exhibit clear assignment to their habitat of origin, with limited, asymmetric gene flow from sulfidic into nonsulfidic populations.

We also conducted *in situ* reciprocal translocation experiments of wild-caught, adult fish, which explicitly tested for local adaptation³³ and natural selection against migrants.³⁴ We found strong, habitat-specific differences in the survival of sulfidic and nonsulfidic populations of each lineage (Figure 4B; binomial generalized linear mixed model [GLMM]; habitat of origin \times testing habitat: $p < 0.001$; Table S3). Fish tested in their own habitat had significantly higher survival rates (88%–100%) than

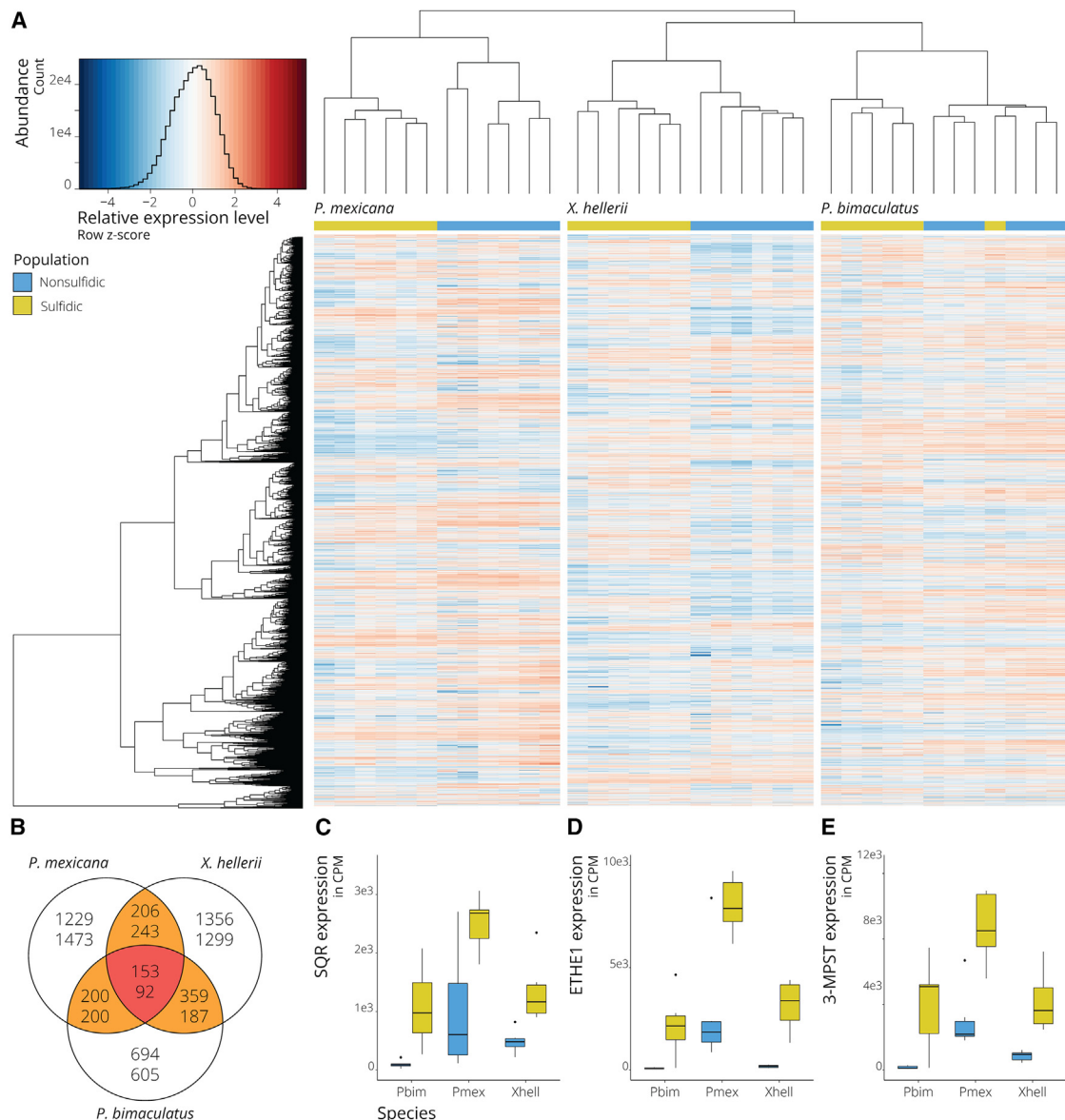


Figure 3. Convergent shifts in gene expression underlie local adaptation

(A) Hierarchical clustering analysis indicates that gene expression profiles cluster by habitat type within each species. Each row represents expression data for one gene, and each column corresponds to an individual. Genes with higher relative expression in individuals from sulfidic habitats are indicated in red, genes with lower relative expression in blue.

(B) Venn diagram showing the number of differentially expressed genes between the sulfidic and nonsulfidic populations of each species and those shared among species. Top numbers are genes upregulated in the sulfidic habitat; bottom numbers are downregulated genes. A list of differentially expressed genes is provided in [Data S1](#) and their corresponding GO annotations in [Data S2](#).

(C–E) Sulfidic populations consistently exhibit higher expression of key H₂S detoxification genes (SQR, sulfide:quinone oxidoreductase; ETHE1, persulfide dioxygenase; 3-MPST, 3-mercaptopyruvate sulfurtransferase) than nonsulfidic populations of the same species. Boxplots of counts per million (CPM) by population. All boxplots have the following elements: center line, median; box limits, upper and lower quartiles; whiskers, $\times 1.5$ interquartile range; points, outliers closed circles.

those tested in the opposite habitat type, with the lowest survival observed for fish moved from the nonsulfidic into the sulfidic habitat (0%–21%). Fish moved from the sulfidic into the nonsulfidic habitat had comparatively high survival (68%–84%)—though significantly lower than resident nonsulfidic fish—ultimately supporting the observed asymmetry of gene flow between habitat types. Overall, this experiment supported the

inference of local adaptation and that natural selection against migrants likely serves as a strong mechanism generating population structure between sulfidic and nonsulfidic populations. Migration of nonsulfidic fish into the sulfide spring is likely mediated by the presence of H₂S and hypoxia. However, it remains unclear why sulfidic fish also face reduced survival in nonsulfidic waters. Previous studies have hypothesized that exposure to the

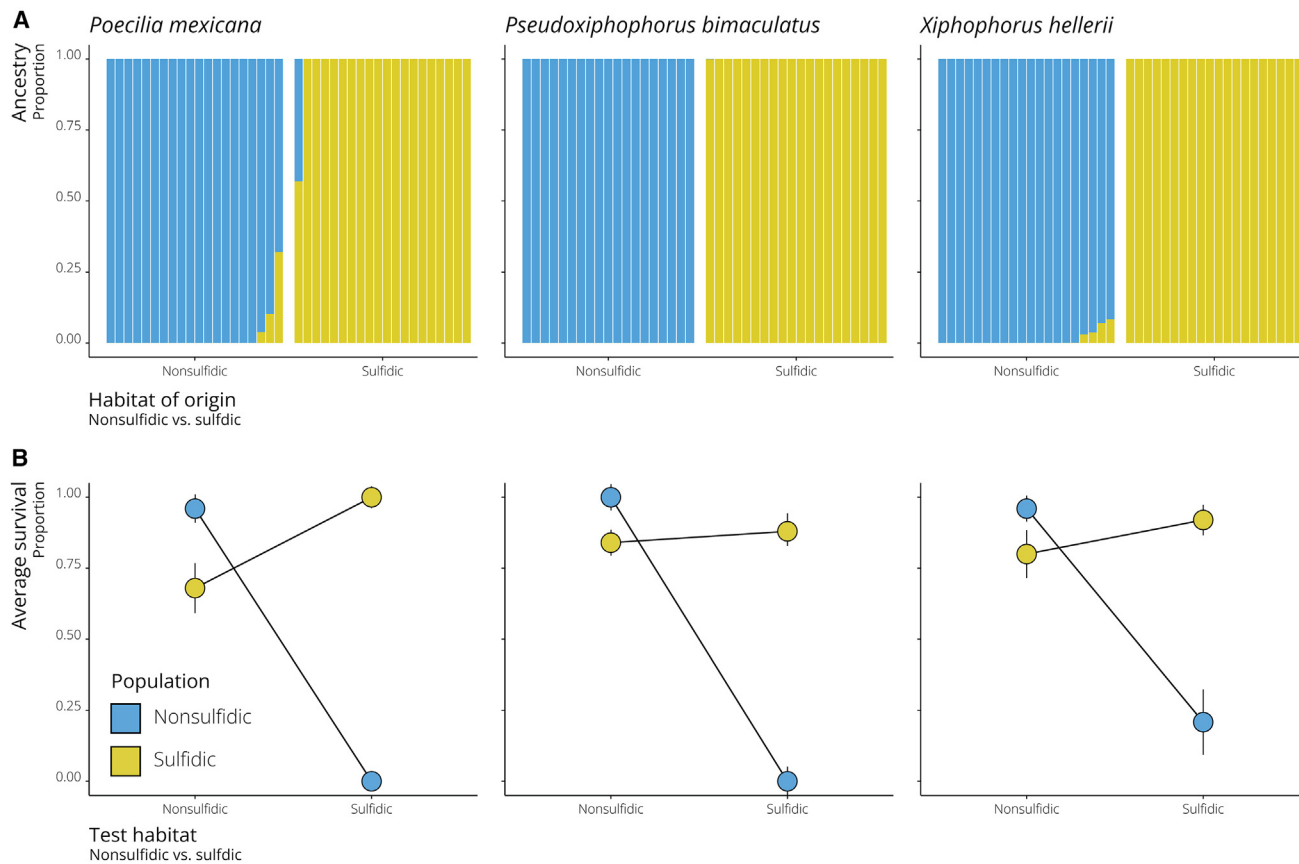


Figure 4. Nonsulfidic and sulfidic populations of three sympatric species exhibit limited gene flow between habitats mediated by strong natural selection against migrants

(A) Admixture analyses revealed substantial population genetic differentiation in each population pair. Individuals are grouped by sampling site, corresponding with the detected genetic population clusters ($K = 2$) shown in blue (nonsulfidic) and yellow (sulfidic). These results were corroborated by principal component (Figure S3) and demographic analyses (Figure S4).

(B) Translocation experiments revealed strong selection against migrants, especially those from nonsulfidic to sulfidic habitats (Table S3). Fish were transferred between sites (test habitat) to estimate survival of migrants between habitats, with individuals collected from the nonsulfidic population in blue and from the sulfidic population in yellow. Error bars represent standard errors of the mean.

normoxic environment could result in oxidative stress,²⁰ or energy limitation in sulfide spring fishes could generally constrain acclimatization to the radically different environmental conditions in nonsulfidic streams.³⁵

Landscape of genomic divergence

The explicit biochemical and physiological effects of H_2S —along with the convergent changes at the transcriptome level—predict clear targets of selection at the genomic level. We first explored potential convergent changes in the mitochondrial genome, which includes genes for three subunits of H_2S ’s primary toxicity target (COX). Mitochondrial haplotype networks revealed that sulfidic populations harbor mitochondrial lineages that are highly divergent from those in the nonsulfidic populations (Figure 5A). Consistent with the asymmetric patterns of gene flow, we found sulfidic mitochondrial haplotypes in nonsulfidic habitats, especially in *P. mexicana* and *X. hellerii*, while nonsulfidic mitochondrial haplotypes were not found in sulfidic populations (except for one apparent first-generation hybrid in *P. mexicana* described above). Using analyses of molecular evolution, we

detected evidence for positive selection (elevated nonsynonymous to synonymous substitution rates, ω ; likelihood-ratio test, $p < 0.01$; Table S4) acting on five mitochondrial genes in all three sulfidic populations, including two COX subunits (COX1 and COX3) and genes encoding subunits of OxPhos complexes I (ND2 and ND3) and III (CYTB), corroborating previous analyses of sulfide spring fishes.^{22,26}

Unlike in the mitochondrial genome, recombination in the nuclear genome can mediate highly heterogeneous divergence during local adaptation. When few genomic regions are directly involved in adaptation, these regions often exhibit disproportionately high divergence (genomic islands of divergence) against a background of regions of low divergence that is homogenized by gene flow.^{36,37} If the observed convergent phenotypic and transcriptomic differentiation had a convergent genomic basis across lineages, we would predict overlapping genomic islands of divergence between sulfidic and nonsulfidic populations across the three species, including regions with mitochondrially functioning genes that are involved in H_2S toxicity and detoxification. Considering the evidence for positive selection on

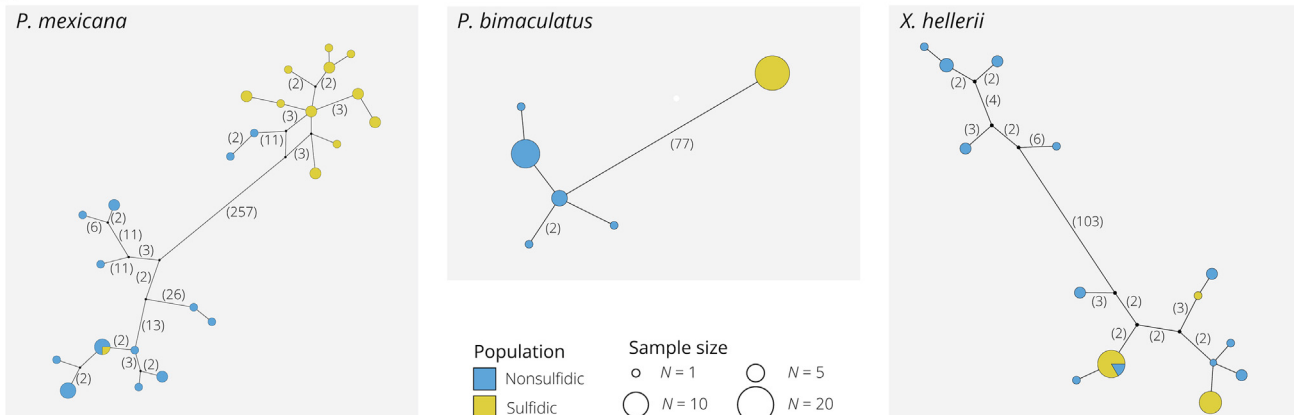
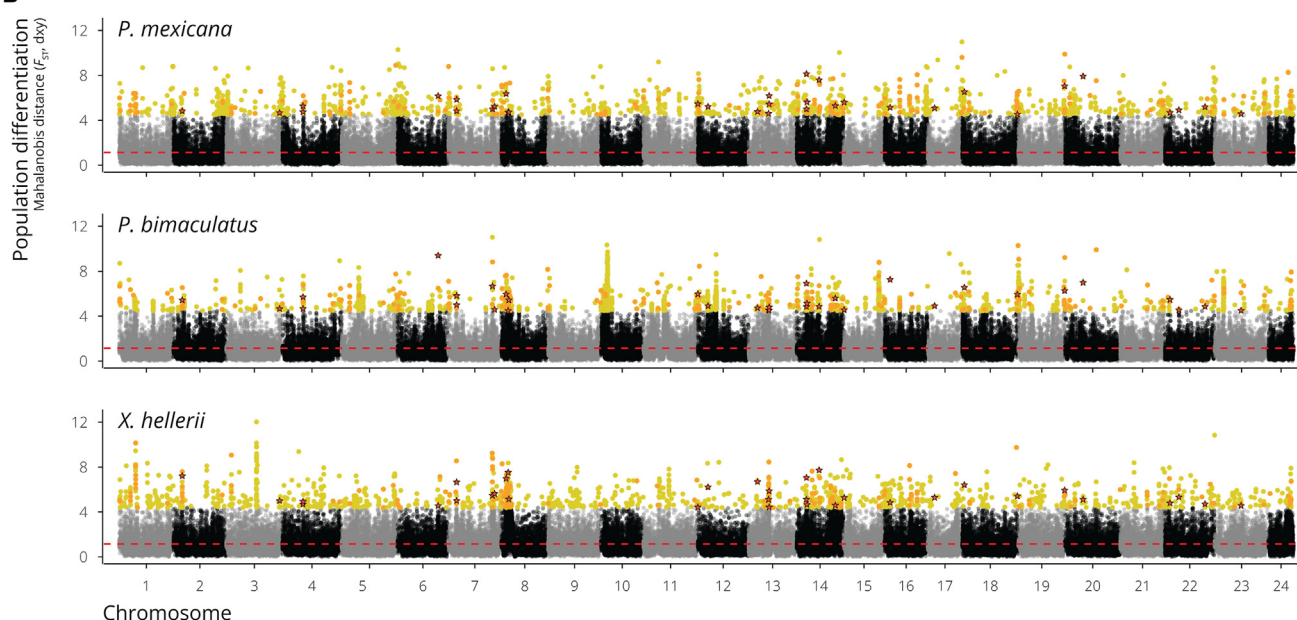
A**B**

Figure 5. Convergent patterns of genomic adaptation are limited to the mitochondrial genome and a few nuclear loci

(A) Haplotype networks based on concatenated mitochondrial genes indicate high levels of mitochondrial divergence between nonsulfidic (blue) and sulfidic (yellow) populations, with asymmetrical introgression of sulfidic mitochondria into nonsulfidic individuals. The relative size of each circle indicates the number of individuals with a particular mitochondrial haplotype, while numbers in parentheses represent the total number of nucleotide differences between haplotypes. Note that several genes in the mitochondrial genome were under positive selection (Table S4).

(B) Mahalanobis distance ($-\log_{10} p$ values of F_{ST} and d_{XY} ; see Figure S5 for plots of raw values) of non-overlapping 5-kb windows across the genome as a measurement of genomic divergence driven by natural selection. Outlier windows (top 1%) unique to each population pair are shown in yellow, while those shared between two population pairs are in orange. The outlier windows shared among all three population pairs are denoted with red stars. A list of genes in outlier regions is provided in Data S3 and their corresponding GO annotations in Data S4. Note that complementary analysis of selective sweeps provided similar results (Data S5 and S6).

mitochondrially encoded genes, we also expected to detect evidence for mito-nuclear coevolution,³⁸ with disproportionately high divergence in the nuclear genes encoding subunits of Ox-Phos complexes I, III, and especially IV. To determine whether selection on the same genomic regions underlies convergence to sulfide spring environments, we used the whole-genome resequencing data described above to characterize the landscape of genomic divergence in each population pair using a combination of relative (F_{ST}) and absolute (d_{XY}) divergence metrics in non-overlapping 5-kb windows.^{39,40} Global estimates of relative

divergence varied considerably among species (mean $F_{ST} = 0.23$ for *Poecilia*, 0.06 for *Pseudoxiphophorus*, and 0.03 for *Xiphophorus*; Figure S5), while absolute divergence across the genome was similar (mean $d_{XY} = 0.003$ for *Poecilia*, 0.004 for *Pseudoxiphophorus*, and 0.003 for *Xiphophorus*; Figure S5).

Using a composite analysis that simultaneously considered relative and absolute divergence,⁴¹ we observed heterogeneous divergence across much of the genome within and among population pairs rather than locally pronounced and shared genomic islands of divergence (Figure 5B; Data S3). By identifying the

most differentiated regions between sulfidic and nonsulfidic individuals within each species (top 1% most differentiated windows; 1,341–1,366 5-kb windows per species), we found that regions of elevated divergence were significantly enriched for genes involved in oxygen transport (*Pseudoxiphophorus*) and immune function (*Xiphophorus* and *Poecilia*), including hemoglobins and major histocompatibility complex genes (GO enrichment analysis: FDR < 0.05; although in *Poecilia* this enrichment was non-significant following FDR correction; [Data S4](#)). To test for convergent patterns of differentiation, we identified regions that were among the most differentiated windows across all three species (top 1% most differentiated in each of the three comparisons to account for variation in average genome-wide differentiation across the three comparisons; [Figure 5B](#)). Thirty-four strongly differentiated regions—containing 28 genes—were shared across all 3 species (significantly more than expected by chance; SuperExactTest, $p < 0.0001$), and 102–156 of these regions were shared between pairs of the 3 species ([Data S3](#)). There was no significant enrichment of GO terms in strongly differentiated regions shared among all lineages, and we found no evidence for genes with known roles in H₂S detoxification or processing in regions of elevated divergence within species ([Data S4](#)). We did observe some overlap of shared differentiated regions and differentially expressed genes within each species (150–198 genes), but not more than would be expected by chance (Fisher's exact test, $p = 0.24$ –1.0).

We also carried out site-frequency-spectrum-based scans for selective sweeps⁴² in each sulfidic population and compared putative sweep regions across the three sulfidic and nonsulfidic contrasts. We found no shared selective sweep outlier regions across all three species ([Figure S5](#)), and the small subset of genes shared among pairs of species was not enriched for any biological functions ([Data S5](#)). *Pseudoxiphophorus bimaculatus* exhibited enrichment of both ion transport and oxygen transport genes, as well as evidence for a selective sweep in the region containing SQR, a key H₂S detoxification enzyme ([Data S6](#)). However, neither *P. mexicana* nor *X. hellerii* exhibited any evidence for selective sweeps in regions containing genes related to H₂S, and only *X. hellerii* exhibited limited enrichment for GO terms in sweep regions (plasma membrane associated genes; [Data S6](#)). It is important to note that differences in effective population sizes between sulfidic and nonsulfidic lineages could influence our ability to detect sweeps, as demographic analyses showed that post-divergence effective population size of sulfidic lineages is around 1/3 to 1/10 of the corresponding nonsulfidic lineages ([Figure S4](#)).

DISCUSSION

The three poeciliid fishes that have colonized the La Gloria sulfide spring complex provided an opportunity to examine how distantly related lineages respond to the same sources of divergent selection. This approach helped reveal what aspects of evolutionary responses are repeatable and predictable and how responses vary across biological scales of organization. We found evidence for local adaptation in each of the lineages and detected signatures of convergence in phenotypic traits that span levels of organismal organization. In addition, there was convergent selection on mitochondrially encoded genes

associated with H₂S toxicity. However, evidence for convergence in the nuclear genomes was scant and not associated with genomic regions predicted to respond to selection from H₂S. Hence, landscapes of genomic divergence can be highly idiosyncratic even when species experience the same selective regime in sympatry, suggesting that evolutionary outcomes are contingent on the genomic substrates that selection is acting on. These results also highlight the potential methodological challenges of identifying convergent shifts associated with highly polygenic traits, phenotypic traits that are associated with high genetic redundancy, or traits underpinned by convergent structural variation.

Evidence for convergence in traits associated with adaptation to sulfide springs

Consistent with previous findings,^{43,44} we found significant differences in body shape between sulfidic and nonsulfidic populations of all three lineages at La Gloria, with sulfide spring fishes exhibiting larger heads than those in nonsulfidic habitats. Previous studies have indicated that increased head size in sulfide spring poeciliids reflects a response to selection on oxygen acquisition in the hypoxic sulfide springs, as head size is correlated with increased gill surface area and higher ventilation capacity in sulfide spring populations of *P. mexicana*^{43,45} and other fishes.^{46,47}

Convergent phenotypic differentiation in H₂S tolerance between sulfidic and nonsulfidic fishes was also observed. Sulfide spring populations exhibited higher tolerance to acute H₂S exposure than populations from adjacent nonsulfidic populations, and, accordingly, nonsulfidic fish suffered high mortality when placed into the natural conditions of the sulfide spring. Previous studies have demonstrated that sulfide spring populations of *P. mexicana* exhibit higher tolerance to acute exposures to H₂S, whether it is quantified at a molecular or whole-organism level.^{26,43} Increased tolerance results from modification of the expression and protein-coding sequences of H₂S toxicity and detoxification genes in well-characterized biological pathways.^{22,26} Additionally, our findings supported those of previous studies carried out in more divergent poeciliid lineages occupying sulfide springs across the Neotropics, which indicated that convergent shifts in the expression of H₂S toxicity and detoxification genes is correlated with H₂S tolerance.^{26,48} We found that upregulated genes in the gills of sulfidic populations from all three species were enriched for genes with mitochondrial functions and H₂S processing, including genes demonstrated to exhibit adaptations for processing H₂S (SQR) or resisting its toxicity (COX) in sulfide spring *P. mexicana*.^{22,26} Ultimately, these shared expression patterns across the three sulfide spring populations provide robust support for convergent regulation of genes with known roles in H₂S toxicity and detoxification.

Although these signals of convergence are substantial, we cannot eliminate the possibility that differences in body shape, sulfide tolerance, and gene expression observed in our experiments with wild-caught specimens were at least in part shaped by plastic responses to H₂S exposure rather than evolved differences between populations. Many physiological traits, such as sulfide tolerance and gene expression, are known to exhibit short-term plastic responses to changes in environmental

conditions.³¹ Common-garden rearing of these species will be needed to better understand how genetic differentiation and plasticity interact to shape gene expression patterns observed in nature; however, laboratory rearing of these sulfidic populations has proven difficult (Tobler, personal observation). Previous common-garden experiments of other sulfidic and nonsulfidic *P. mexicana* populations, notably less divergent than the populations examined in this study, have provided evidence for a heritable basis to multiple morphological traits, metabolic rates, sulfide tolerance, and expression variation in H₂S-processing and OxPhos-related genes.^{31,32,49,50} Furthermore, our population genetic analyses demonstrated that fish collected from the sulfidic and nonsulfidic habitat exhibit very little gene flow between them, despite the possibility of panmixia due to the connectedness of the streams in which they are found, suggesting that the phenotypic differentiation we observed likely does not solely reflect habitat-specific inducible effects but is at least in part the result of evolved differences.

Genetic basis of adaptation

Even with clear evidence for convergent phenotypic responses to shared environmental conditions, we found that patterns of convergence were not consistent across scales of biological organization. Specifically, we found limited evidence for convergent evolution at the genomic level, suggesting that convergence in morphology, physiological tolerance, and gene expression do not simply stem from genomic differentiation at one, or few, genomic loci. Our results show that nuclear genes typically implicated in H₂S adaptation were not associated with shared or species-specific outlier regions, including genes of the SQR pathway that are involved in enzymatic H₂S detoxification and nuclear genes associated with COX and other OxPhos components. These results stand in stark contrast to previous investigations of replicated *P. mexicana* populations adapted to sulfide springs across southern Mexico, where a variety of approaches have demonstrated predictable evolution of genes with known roles in H₂S detoxification and energy metabolism.^{22,24,25} This high level of convergence among closely related populations paired with the limited convergence observed among divergent lineages in the present study suggests that even the strong physiological demands of H₂S toxicity are not sufficient to constrain adaptation to one or a few solutions at the genomic level. Rather, access to shared pools of genetic variation, as is the case for replicated *P. mexicana* populations,^{24,27} appears to facilitate convergence at the genomic level. These results align with previous studies investigating genome-wide patterns of changes in protein-coding sequences (based on transcriptomic data), which found little evidence for convergent evolution of protein-coding sequences outside of the mitochondrial genome.²⁶ However, in line with previous studies, we did observe consistent modification of genes encoded by the mitochondrial genome across all three sulfidic populations, including the direct targets of H₂S toxicity (COX subunits). Additionally, nonsulfidic mitochondrial haplotypes were not found in individuals sampled from the sulfidic habitat (except for one apparent F1 hybrid), suggesting a critical role of mitochondrial DNA in mediating survival in the toxic conditions. Despite evidence for selection on mitochondrial genes,⁵¹ it remains unclear how genetic variation in mitochondrial vs. nuclear loci contribute

to adaptive variation in OxPhos function. The evolution of H₂S-resistance could be largely driven by modification of mitochondrial COX subunits that form the reactive center of the protein and without coevolutionary changes in the corresponding nuclear subunits. This finding challenges the general paradigm that adaptation of mitochondrial function coincides with mito-nuclear coevolution.⁵¹

Although evidence for selection on nuclear genes associated with H₂S detoxification and OxPhos was sparse, functional annotation of shared and unique outlier regions did find limited evidence for enrichment of genes involved in oxygen transport and immune function (Data S4). Evidence for selection on oxygen transport proteins such as hemoglobin is not surprising, as H₂S is capable of binding to and impairing hemeprotein function.^{52,53} The presence of hemoglobin genes in outlier regions also confirms findings of positive selection on hemoglobin genes in other sulfide spring poeciliids.⁵⁴ In contrast, the large number of genes associated with immune function was not expected, although immune genes are known hotspots for selection in vertebrates.⁵⁵ Selection on immune genes could be driven by differences in parasite and pathogen communities between sulfidic and nonsulfidic habitats, which have been documented in other sulfide springs inhabited by poeciliid fish.^{56,57} Alternatively, there have been long-standing hypotheses about the potential role of H₂S-oxidizing microsymbionts in adaptation to sulfide spring environments.^{16,58} Recent studies have indeed documented convergent changes in gut microbiomes of fish from sulfidic habitats, including microbes that have been implicated in mediating host adaptation to H₂S in other animals.⁵⁹ Hence, changes in host-microbe interactions upon sulfide spring colonization may also exert selection on immune genes.⁶⁰

Even though H₂S has clear-cut biochemical and physiological effects, tolerance to this toxicant involves numerous genes. OxPhos complexes alone contain over 80 nuclear-encoded genes,⁶¹ and dozens of genes contribute to the physiological processing of H₂S and other sulfur compounds.^{62,63} For this reason, the lack of convergence we observed at the genome level could be the result of the polygenic nature of H₂S tolerance, which is known to pose substantial challenges for detecting patterns of genomic convergence because associated loci are unlikely to form large islands of divergence but rather be scattered throughout the genome. It is possible that subtle allele frequency shifts across multiple polymorphic OxPhos or H₂S processing genes could result in adaptive modifications to these pathways without leaving a molecular signature detectable by scans for genomic differentiation between divergent species pairs.^{64,65} Such subtle allele frequency shifts are now detectable when closely related populations with shared allelic variants are exposed to similar sources of selection,⁶⁶ and they have revealed evidence for some genomic convergence even in polygenic traits^{7,67,68}; however, these methods are not applicable to the highly divergent population pairs that were investigated here.

Alternatively, the absence of genomic convergence may not just be a consequence of our inability to detect it but a real phenomenon that could be explained by several mechanisms. First, there may be genetic redundancy in H₂S tolerance, where many different combinations of alleles throughout the genome can underpin the same phenotype. If genetic redundancy is high, lineage-specific responses to selection that are in part shaped by

historical contingencies^{69–71} may underpin the convergence signatures of phenotypic traits and gene expression without genomic convergence across species.⁷² Second, the environmental differences between sulfidic and adjacent nonsulfidic habitats are complex (Figure 1C). The multifarious sources of selection have caused adaptive modifications of whole suites of complex traits beyond H₂S tolerance, and most of these traits likely have different genomic bases.¹⁹ Despite the signals of convergence we documented in different phenotypes, trait optima may be different for each of the species, both because phenotypic integration creates complex interactions among traits^{73–75} and because the three species seem to occupy different microhabitats within the spring (Figure S2). Variation in trait combinations among species and unquantified niche differences may in turn favor nonconvergent genomic solutions.² Finally, the absence of convergence may have been influenced by differences in demographic histories. *Poecilia mexicana* has colonized the sulfide spring significantly earlier than the other two species (~19,000 years vs. ~11,000 years for *P. bimaculatus* and ~7,500 years for *X. hellerii*), and there is significant variation in effective population sizes and relative migration rates from nonsulfidic to sulfidic habitats (Figure S4).

Overall, adaptation to H₂S may primarily be driven by changes in mitochondrial protein function and the expression of detoxification genes, with lineage-specific mechanisms producing the convergent gene expression patterns uncovered by transcriptome analyses. Because differentially expressed genes were not overrepresented in the outlier genome regions, as might be expected by selection acting on *cis*-regulatory elements,²⁵ outlier regions may harbor *trans*-regulatory elements mediating adaptive shifts in gene expression.⁷⁶ Divergent selection acting on regulatory elements has been implicated in adaptive divergence for several well-known models in evolutionary ecology.^{77–79} The problem of detecting the genetic basis of trait variation by any of the above means can be exacerbated when adaptive evolution gives rise to reproductive isolation. Selection on small-effect loci spread across the genome can facilitate strong and stable reductions in gene flow over short timescales,^{80,81} similar to the reduced gene flow observed for all three lineages in our study. High levels of background divergence resulting from post-speciation divergence can further obscure the signatures of selection on the loci mediating adaptation during earlier stages of divergence.^{82–84}

Conclusions

Although convergent evolution in response to shared selective pressure is present across diverse lineages, our results showed that patterns of convergence in response to extreme environments are not consistent across levels of biological organization. We also demonstrated that mechanistically linking strong signals of convergence in morphology, physiology, and gene expression to genomic variation is challenging due to the magnitude of ways in which different aspects of genomic variation interplay to affect phenotypic variation. Although we observed signatures of independent local adaptation and reproductive isolation between sulfidic and nonsulfidic populations in three highly divergent lineages, variation in the complexity and genomic architecture of traits and the degree of genetic redundancy may reduce our ability to confidently identify signals of convergence at the

genome level. Although substantial progress has been made in understanding the molecular basis of trait evolution, methodological and statistical limitations are prevalent when traits are complex, leading to an underrepresentation of studies covering the adaptation of non-model organisms to complex ecological stressors.

RESOURCE AVAILABILITY

Lead contact

Requests for further information should be directed to the lead contact, Michael Tobler (tobler@umsl.edu).

Materials availability

This study did not generate new reagents.

Data and code availability

All data associated with this manuscript have been deposited on Dryad⁸⁵ or GenBank (DNA: NCBI BioProject PRJNA738871; RNA: NCBI BioProject PRJNA608180 and PRJNA1152527). This manuscript does not report original code.

ACKNOWLEDGMENTS

We are indebted to the community of Teapa, especially the owners of Rancho La Gloria, for providing access to study sites and to the Centro de Investigación e Innovación para la Enseñanza y Aprendizaje (CIEIA) for their hospitality and support during the nearly decade-long course of this project. We thank N. Barts, C. Carson, Z. Cumber, T. Doumas, G.W. Hopper, C. N. Passow, and E.A. Renner for assistance in the field, as well as O. Cornejo, K.B. Gido, A.G. Hope, D.A. Marques, and T.J. Morgan for their comments and discussions. All procedures involving animals were approved by the Institutional Animal Care and Use Committee of Kansas State University (protocols 3473, 3992, 4585, and 4586), and the Mexican government provided permits for fieldwork (SGPA/DGVS/04315/11, DGOPA.09004.041111.3088, PRMN/DGOPA-003/2014, PRM/DGOPA-009/2015, and PRMN/DGOPA-012/2017). This work was supported by grants from the NSF (IOS-1557860, IOS-1931657, IOS-2311366, and IOS-2423844) and the US Army Research Office (W911NF-15-1-0175, W911NF-16-1-0225) to J.L.K. and M.T. R.G. was supported by the American Museum of Natural History (Theodore Roosevelt Memorial Fund grant), Friends of Sunset Zoo (Conservation Scholar Program), American Live-bearer Association (Vern Parish Fund award), Society for the Study of Evolution (Rosemary Grant Advanced Graduate Research Excellence Grant), American Society of Naturalists (Student Research Award), and a NSF Graduate Research Fellowship (DGE-1746899). M.T. was supported by the Des Lee Collaborative Vision in Zoological Studies.

AUTHOR CONTRIBUTIONS

Conceptualization: R.G., L.A.-R., J.L.K., and M.T. Investigation: R.G., H.C., L.A.-R., J.L.K., and M.T. Formal analysis: R.G., A.P.B., C.D., K.L.M., J.N., J.L.K., and M.T. Data curation: R.G., J.L.K., and M.T. Writing – original draft: R.G., J.L.K., and M.T. Writing – review & editing: R.D.-K., J.L.K., and M.T. Visualization: M.T. Supervision, project administration, and funding acquisition: J.L.K. and M.T.

DECLARATION OF INTERESTS

The authors declare no competing interests.

STAR METHODS

Detailed methods are provided in the online version of this paper and include the following:

- KEY RESOURCES TABLE
- EXPERIMENTAL MODEL AND SUBJECT DETAILS

- **METHOD DETAILS**
 - Water chemistry
 - Body shape
 - Tolerance to acute H₂S exposure
 - Gene expression variation
 - Genome sequencing
 - Reciprocal translocation experiment
- **QUANTIFICATION AND STATISTICAL ANALYSIS**
 - Analysis of body shape
 - Analysis of tolerance to acute H₂S exposure
 - Analysis of gene expression variation
 - Analysis of genome sequencing
 - Analysis of reciprocal translocation experiment

SUPPLEMENTAL INFORMATION

Supplemental information can be found online at <https://doi.org/10.1016/j.cub.2024.09.027>.

Received: December 13, 2023

Revised: July 18, 2024

Accepted: September 11, 2024

Published: October 11, 2024

REFERENCES

1. Schlüter, D., and Nagel, L.M. (1995). Parallel speciation by natural selection. *Am. Nat.* 146, 292–301. <https://doi.org/10.1086/285799>.
2. Kaeuffer, R., Peichel, C.L., Bolnick, D.I., and Hendry, A.P. (2012). Parallel and nonparallel aspects of ecological, phenotypic, and genetic divergence across replicate population pairs of lake and stream stickleback. *Evolution* 66, 402–418. <https://doi.org/10.1111/j.1558-5646.2011.01440.x>.
3. Blount, Z.D., Lenski, R.E., and Losos, J.B. (2018). Contingency and determinism in evolution: replaying life's tape. *Science* 362, eaam5979. <https://doi.org/10.1126/science.aam5979>.
4. Rosenblum, E.B., Parent, C.E., and Brandt, E.E. (2014). The molecular basis of phenotypic convergence. *Annu. Rev. Ecol. Evol. Syst.* 45, 203–226. <https://doi.org/10.1146/annurev-ecolsys-120213-091851>.
5. Colosimo, P.F., Hosemann, K.E., Balabhadra, S., Villarreal, G., Dickson, M., Grimwood, J., Schmutz, J., Myers, R.M., Schlüter, D., and Kingsley, D.M. (2005). Widespread parallel evolution in sticklebacks by repeated fixation of ectodysplasin alleles. *Science* 307, 1928–1933. <https://doi.org/10.1126/science.1107239>.
6. Rosenblum, E.B., Römler, H., Schöneberg, T., and Hoekstra, H.E. (2010). Molecular and functional basis of phenotypic convergence in white lizards at White Sands. *Proc. Natl. Acad. Sci. USA* 107, 2113–2117. <https://doi.org/10.1073/pnas.0911042107>.
7. Chaturvedi, S., Gompert, Z., Feder, J.L., Osborne, O.G., Muschick, M., Riesch, R., Soria-Carrasco, V., and Nosil, P. (2022). Climatic similarity and genomic background shape the extent of parallel adaptation in *Timema* stick insects. *Nat. Ecol. Evol.* 6, 1952–1964. <https://doi.org/10.1038/s41559-022-01909-6>.
8. Yearman, S., Hodgins, K.A., Lotterhos, K.E., Suren, H., Nadeau, S., Degner, J.C., Nurkowski, K.A., Smets, P., Wang, T., Gray, L.K., et al. (2016). Convergent local adaptation to climate in distantly related conifers. *Science* 353, 1431–1433. <https://doi.org/10.1126/science.aaf7812>.
9. Conte, G.L., Arnegard, M.E., Peichel, C.L., and Schlüter, D. (2012). The probability of genetic parallelism and convergence in natural populations. *Proc. Biol. Sci.* 279, 5039–5047. <https://doi.org/10.1098/rspb.2012.2146>.
10. Soria-Carrasco, V., Gompert, Z., Comeault, A.A., Farkas, T.E., Parchman, T.L., Johnston, J.S., Buerkle, C.A., Feder, J.L., Bast, J., Schwander, T., et al. (2014). Stick insect genomes reveal natural selection's role in parallel speciation. *Science* 344, 738–742. <https://doi.org/10.1126/science.1252136>.
11. Stuart, Y.E., Veen, T., Weber, J.N., Hanson, D., Ravinet, M., Lohman, B.K., Thompson, C.J., Tasneem, T., Doggett, A., Izen, R., et al. (2017). Contrasting effects of environment and genetics generate a continuum of parallel evolution. *Nat. Ecol. Evol.* 1, 0158. <https://doi.org/10.1038/s41559-017-0158>.
12. Morales, H.E., Faria, R., Johannesson, K., Larsson, T., Panova, M., Westram, A.M., and Butlin, R.K. (2019). Genomic architecture of parallel ecological divergence: Beyond a single environmental contrast. *Sci. Adv.* 5, eaav9963. <https://doi.org/10.1126/sciadv.aav9963>.
13. Rosenblum, E.B., and Harmon, L.J. (2011). "Same same but different": replicated ecological speciation at White Sands. *Evolution* 65, 946–960. <https://doi.org/10.1111/j.1558-5646.2010.01190.x>.
14. Raeymaekers, J.A.M., Chaturvedi, A., Hablützel, P.I., Verdonck, I., Hellemans, B., Maes, G.E., De Meester, L., and Volckaert, F.A.M. (2017). Adaptive and non-adaptive divergence in a common landscape. *Nat. Commun.* 8, 267. <https://doi.org/10.1038/s41467-017-00256-6>.
15. Weber, A.A.-T., Rajkov, J., Smailus, K., Egger, B., and Salzburger, W. (2021). Speciation dynamics and extent of parallel evolution along a lake-stream environmental contrast in African cichlid fishes. *Sci. Adv.* 7, eabg5391. <https://doi.org/10.1126/sciadv.abg5391>.
16. Tobler, M., Passow, C.N., Greenway, R., Kelley, J.L., and Shaw, J.H. (2016). The evolutionary ecology of animals inhabiting hydrogen sulfide-rich environments. *Annu. Rev. Ecol. Syst.* 47, 239–262. <https://doi.org/10.1146/annurev-ecolsys-121415-032418>.
17. Cooper, C.E., and Brown, G.C. (2008). The inhibition of mitochondrial cytochrome oxidase by the gases carbon monoxide, nitric oxide, hydrogen cyanide and hydrogen sulfide: chemical mechanism and physiological significance. *J. Bioenerg. Biomembr.* 40, 533–539. <https://doi.org/10.1007/s10863-008-9166-6>.
18. Reznick, D.N., Furness, A.I., Meredith, R.W., and Springer, M.S. (2017). The origin and biogeographic diversification of fishes in the family Poeciliidae. *PLoS One* 12, e0172546. <https://doi.org/10.1371/journal.pone.0172546>.
19. Tobler, M., Kelley, J.L., Plath, M., and Riesch, R. (2018). Extreme environments and the origins of biodiversity: adaptation and speciation in sulphide spring fishes. *Mol. Ecol.* 27, 843–859. <https://doi.org/10.1111/mec.14497>.
20. Plath, M., Pfenniger, M., Lerp, H., Riesch, R., Eschenbrenner, C., Slattery, P.A., Bierbach, D., Herrmann, N., Schulte, M., Arias-Rodriguez, L., et al. (2013). Genetic differentiation and selection against migrants in evolutionarily replicated extreme environments. *Evolution* 67, 2647–2661. <https://doi.org/10.1111/evo.12133>.
21. Riesch, R., Tobler, M., Lerp, H., Jourdan, J., Doumas, T., Nosil, P., Langerhans, R.B., and Plath, M. (2016). Extremophile Poeciliidae: multivariate insights into the complexity of speciation along replicated ecological gradients. *BMC Evol. Biol.* 16, 136. <https://doi.org/10.1186/s12862-016-0705-1>.
22. Pfenniger, M., Lerp, H., Tobler, M., Passow, C., Kelley, J.L., Funke, E., Greshake, B., Erkoc, U.K., Berberich, T., and Plath, M. (2014). Parallel evolution of cox genes in H₂S-tolerant fish as key adaptation to a toxic environment. *Nat. Commun.* 5, 3873. <https://doi.org/10.1038/ncomms4873>.
23. Pfenniger, M., Patel, S., Arias-Rodriguez, L., Feldmeyer, B., Riesch, R., and Plath, M. (2015). Unique evolutionary trajectories in repeated adaptation to hydrogen sulphide-toxic habitats of a neotropical fish (*Poecilia mexicana*). *Mol. Ecol.* 24, 5446–5459. <https://doi.org/10.1111/mec.13397>.
24. Brown, A.P., McGowan, K.L., Schwarzkopf, E.J., Greenway, R., Rodriguez, L.A., Tobler, M., and Kelley, J.L. (2019). Local ancestry analysis reveals genomic convergence in extremophile fishes. *Philos. Trans. R. Soc. Lond. B Biol. Sci.* 374, 20180240. <https://doi.org/10.1098/rstb.2018.0240>.
25. Brown, A.P., Arias-Rodriguez, L., Yee, M.-C., Tobler, M., and Kelley, J.L. (2018). Concordant changes in gene expression and nucleotides underlie

independent adaptation to hydrogen-sulfide-rich environments. *Genome Biol. Evol.* 10, 2867–2881. <https://doi.org/10.1093/gbe/evy198>.

26. Greenway, R., Barts, N., Henpita, C., Brown, A.P., Arias Rodriguez, L., Rodríguez Peña, C.M., Arndt, S., Lau, G.Y., Murphy, M.P., Wu, L., et al. (2020). Convergent evolution of conserved mitochondrial pathways underlies repeated adaptation to extreme environments. *Proc. Natl. Acad. Sci. USA* 117, 16424–16430. <https://doi.org/10.1073/pnas.2004223117>.
27. Ryan, K., Greenway, R., Landers, J., Arias-Rodriguez, L., Tobler, M., and Kelley, J.L. (2023). Selection on standing genetic variation mediates convergent evolution in extremophile fish. *Mol. Ecol.* 32, 5042–5054. <https://doi.org/10.1111/mec.17081>.
28. De-Kayne, R., Perry, B.W., McGowan, K.L., Landers, J., Arias-Rodriguez, L., Greenway, R., Rodríguez Peña, C.M., Tobler, M., and Kelley, J.L. (2024). Evolutionary rate shifts in coding and regulatory regions underpin repeated adaptation to sulfidic streams in poeciliid fishes. *Genome Biol. Evol.* 16, evae087. <https://doi.org/10.1093/gbe/evae087>.
29. Tobler, M., and Plath, M. (2011). Living in extreme habitats. In *Ecology and Evolution of Poeciliid Fishes*, J. Evans, A. Pilastro, and I. Schlupp, eds. (University of Chicago Press), pp. 120–127.
30. Wang, M., Zhao, Y., and Zhang, B. (2015). Efficient Test and Visualization of Multi-Set Intersections. *Sci. Rep.* 5, 16923. <https://doi.org/10.1038/srep16923>.
31. Passow, C.N., Henpita, C., Shaw, J.H., Quackenbush, C.R., Warren, W.C., Schartl, M., Arias-Rodriguez, L., Kelley, J.L., and Tobler, M. (2017). The roles of plasticity and evolutionary change in shaping gene expression variation in natural populations of extremophile fish. *Mol. Ecol.* 26, 6384–6399. <https://doi.org/10.1111/mec.14360>.
32. Tobler, M., Henpita, C., Bassett, B., Kelley, J.L., and Shaw, J.H. (2014). H₂S exposure elicits differential expression of candidate genes in fish adapted to sulfidic and non-sulfidic environments. *Comp. Biochem. Physiol. A Mol. Integr. Physiol.* 175, 7–14. <https://doi.org/10.1016/j.cbpa.2014.04.012>.
33. Kawecki, T.J., and Ebert, D. (2004). Conceptual issues in local adaptation. *Ecol. Lett.* 7, 1225–1241. <https://doi.org/10.1111/j.1461-0248.2004.00684.x>.
34. Nosil, P., Vines, T.H., and Funk, D.J. (2005). Perspective: Reproductive isolation caused by natural selection against immigrants from divergent habitats. *Evolution* 59, 705–719.
35. Passow, C.N., Arias-Rodriguez, L., and Tobler, M. (2017). Convergent evolution of reduced energy demands in extremophile fish. *PLoS One* 12, e0186935. <https://doi.org/10.1371/journal.pone.0186935>.
36. Ravinet, M., Faria, R., Butlin, R.K., Galindo, J., Bierne, N., Rafajlović, M., Noor, M.A.F., Mehlig, B., and Westram, A.M. (2017). Interpreting the genomic landscape of speciation: a road map for finding barriers to gene flow. *J. Evol. Biol.* 30, 1450–1477. <https://doi.org/10.1111/jeb.13047>.
37. Nosil, P., and Feder, J.L. (2012). Genomic divergence during speciation: causes and consequences. *Philos. Trans. R. Soc. Lond. B Biol. Sci.* 367, 332–342. <https://doi.org/10.1098/rstb.2011.0263>.
38. Rand, D.M., Haney, R.A., and Fry, A.J. (2004). Cytonuclear coevolution: the genomics of cooperation. *Trends Ecol. Evol.* 19, 645–653. <https://doi.org/10.1016/j.tree.2004.10.003>.
39. Cruckshank, T.E., and Hahn, M.W. (2014). Reanalysis suggests that genomic islands of speciation are due to reduced diversity, not reduced gene flow. *Mol. Ecol.* 23, 3133–3157. <https://doi.org/10.1111/mec.12796>.
40. Verity, R., Collins, C., Card, D.C., Schaal, S.M., Wang, L., and Lotterhos, K.E. (2017). minotaur: A platform for the analysis and visualization of multivariate results from genome scans with R Shiny. *Mol. Ecol. Resour.* 17, 33–43. <https://doi.org/10.1111/1755-0998.12579>.
41. Lotterhos, K.E., Card, D.C., Schaal, S.M., Wang, L., Collins, C., and Verity, B. (2017). Composite measures of selection can improve the signal-to-noise ratio in genome scans. *Methods Ecol. Evol.* 8, 717–727. <https://doi.org/10.1111/2041-210X.12774>.
42. Chen, H., Patterson, N., and Reich, D. (2010). Population differentiation as a test for selective sweeps. *Genome Res.* 20, 393–402. <https://doi.org/10.1101/gr.100545.109>.
43. Tobler, M., Palacios, M., Chapman, L.J., Mitrofanov, I., Bierbach, D., Plath, M., Arias-Rodriguez, L., de León, F.J.G., and Mateos, M. (2011). Evolution in extreme environments: replicated phenotypic differentiation in livebearing fish inhabiting sulfidic springs. *Evolution* 65, 2213–2228. <https://doi.org/10.1111/j.1558-5646.2011.01298.x>.
44. Tobler, M., and Hastings, L. (2011). Convergent patterns of body shape differentiation in four different clades of poeciliid fishes inhabiting sulfide springs. *Evol. Biol.* 38, 412–421. <https://doi.org/10.1007/s11692-011-9129-4>.
45. Camarillo, H., Arias Rodriguez, L., and Tobler, M. (2020). Functional consequences of phenotypic variation between locally adapted populations: swimming performance and ventilation in extremophile fish. *J. Evol. Biol.* 33, 512–523. <https://doi.org/10.1111/jeb.13586>.
46. Langerhans, R.B., Chapman, L.J., and DeWitt, T.J. (2007). Complex phenotype-environment associations revealed in an East African cyprinid. *J. Evol. Biol.* 20, 1171–1181. <https://doi.org/10.1111/j.1420-9101.2007.01282.x>.
47. Chapman, L.G., Galis, F., and Shinn, J. (2000). Phenotypic plasticity and the possible role of genetic assimilation: hypoxia-induced trade-offs in the morphological traits of an African cichlid. *Ecol. Lett.* 3, 387–393. <https://doi.org/10.1046/j.1461-0248.2000.00160.x>.
48. Kelley, J.L., Arias-Rodriguez, L., Patacsil Martin, D., Yee, M.-C., Bustamante, C.D., and Tobler, M. (2016). Mechanisms underlying adaptation to life in hydrogen sulfide-rich environments. *Mol. Biol. Evol.* 33, 1419–1434. <https://doi.org/10.1093/molbev/msw020>.
49. Barts, N. (2020). Comparative physiology and the predictability of evolution in extreme environments. PhD thesis (Kansas State University).
50. Nobrega, M., Greenway, R., Passow, C.N., Arias Rodriguez, L., and Tobler, M. (2024). Effects of plasticity and genetic divergence in phenotypic trait expression of sulfide spring fishes. *Environ. Biol. Fishes* 107, 611–629. <https://doi.org/10.1007/s10641-024-01555-w>.
51. Hill, G.E. (2015). Mitonuclear Ecology. *Mol. Biol. Evol.* 32, 1917–1927. <https://doi.org/10.1093/molbev/msv104>.
52. Pietri, R., Román-Morales, E., and López-Garriga, J. (2011). Hydrogen sulfide and heme proteins: knowledge and mysteries. *Antioxid. Redox Signal.* 15, 393–404. <https://doi.org/10.1089/ars.2010.3698>.
53. Evans, S.V., Sishta, B.P., Mauk, A.G., and Brayer, G.D. (1994). Three-dimensional structure of cyanomet-sulfmyoglobin C. *Proc. Natl. Acad. Sci. USA* 91, 4723–4726. <https://doi.org/10.1073/pnas.91.11.4723>.
54. Barts, N., Greenway, R., Passow, C.N., Arias Rodriguez, L., Kelley, J.L., and Tobler, M. (2018). Molecular evolution and expression of oxygen transport genes in livebearing fishes (Poeciliidae) from hydrogen sulfide rich springs. *Genome* 61, 273–286. <https://doi.org/10.1139/gen-2017-0051>.
55. Shultz, A.J., and Sackton, T.B. (2019). Immune genes are hotspots of shared positive selection across birds and mammals. *eLife* 8, e41815. <https://doi.org/10.7554/eLife.41815>.
56. Tobler, M., Plath, M., Riesch, R., Schlupp, I., Grasse, A., Munimanda, G.K., Setzer, C., Penn, D.J., and Moodley, Y. (2014). Selection from parasites favours immunogenetic diversity but not divergence among locally adapted host populations. *J. Evol. Biol.* 27, 960–974. <https://doi.org/10.1111/jeb.12370>.
57. Riesch, R., Morley, N.J., Jourdan, J., Arias Rodriguez, L., and Plath, M. (2020). Sulphide-toxic habitats are not refuges from parasite infections in an extremophile fish. *Acta Oecol.* 106, 103602. <https://doi.org/10.1016/j.actao.2020.103602>.
58. Hotaling, S., Quackenbush, C.R., Bennett-Ponsford, J., New, D.D., Arias-Rodriguez, L., Tobler, M., and Kelley, J.L. (2019). Bacterial Diversity in Replicated Hydrogen Sulfide-Rich Streams. *Microb. Ecol.* 77, 559–573. <https://doi.org/10.1007/s00248-018-1237-6>.

59. Wilson, E. (2024). The evolutionary ecology of extremophile fishes from hypersaline lakes, caves, and toxic streams. PhD thesis (Kansas State University).

60. Hooper, L.V., Littman, D.R., and Macpherson, A.J. (2012). Interactions between the microbiota and the immune system. *Science* 336, 1268–1273. <https://doi.org/10.1126/science.1223490>.

61. Zhang, F., and Broughton, R.E. (2013). Mitochondrial-nuclear interactions: compensatory evolution or variable functional constraint among vertebrate oxidative phosphorylation genes? *Genome Biol. Evol.* 5, 1781–1791. <https://doi.org/10.1093/gbe/evt129>.

62. Olson, K.R. (2018). H₂S and polysulfide metabolism: Conventional and unconventional pathways. *Biochem. Pharmacol.* 149, 77–90. <https://doi.org/10.1016/j.bcp.2017.12.010>.

63. Stipanuk, M.H., and Ueki, I. (2011). Dealing with methionine/homocysteine sulfur: cysteine metabolism to taurine and inorganic sulfur. *J. Inherit. Metab. Dis.* 34, 17–32. <https://doi.org/10.1007/s10545-009-9006-9>.

64. Yeaman, S. (2015). Local Adaptation by Alleles of Small Effect. *Am. Nat.* 186, S74–S89. <https://doi.org/10.1086/682405>.

65. Simons, Y.B., Bullaughey, K., Hudson, R.R., and Sella, G. (2018). A population genetic interpretation of GWAS findings for human quantitative traits. *PLoS Biol.* 16, e2002985. <https://doi.org/10.1371/journal.pbio.2002985>.

66. Whiting, J.R., Paris, J.R., van der Zee, M.J., and Fraser, B.A. (2022). AF-vapeR: A multivariate genome scan for detecting parallel evolution using allele frequency change vectors. *Methods Ecol. Evol.* 13, 2167–2180. <https://doi.org/10.1111/2041-210X.13952>.

67. Montejo-Kovacevich, G., Salazar, P.A., Smith, S.H., Gavilanes, K., Bacquet, C.N., Chan, Y.F., Jiggins, C.D., Meier, J.I., and Nadeau, N.J. (2021). Genomics of altitude-associated wing shape in two tropical butterflies. *Mol. Ecol.* 30, 6387–6402. <https://doi.org/10.1111/mec.16067>.

68. Konečná, V., Šustr, M., Požárová, D., Čertner, M., Krejčová, A., Tylová, E., and Kolář, F. (2022). Genomic basis and phenotypic manifestation of (non-)parallel serpentine adaptation in *Arabidopsis arenosa*. *Evolution* 76, 2315–2331. <https://doi.org/10.1111/evo.14593>.

69. Barghi, N., Tobler, R., Nolte, V., Jakšić, A.M., Mallard, F., Otte, K.A., Dolezal, M., Taus, T., Kofler, R., and Schlötterer, C. (2019). Genetic redundancy fuels polygenic adaptation in *Drosophila*. *PLoS Biol.* 17, e3000128. <https://doi.org/10.1371/journal.pbio.3000128>.

70. Barghi, N., Hermission, J., and Schlötterer, C. (2020). Polygenic adaptation: a unifying framework to understand positive selection. *Nat. Rev. Genet.* 21, 769–781. <https://doi.org/10.1038/s41576-020-0250-z>.

71. Láruson, Á.J., Yeaman, S., and Lotterhos, K.E. (2020). The importance of genetic redundancy in evolution. *Trends Ecol. Evol.* 35, 809–822. <https://doi.org/10.1016/j.tree.2020.04.009>.

72. Steiner, C.C., Römpl, H., Boettger, L.M., Schöneberg, T., and Hoekstra, H.E. (2009). The genetic basis of phenotypic convergence in beach mice: similar pigment patterns but different genes. *Mol. Biol. Evol.* 26, 35–45. <https://doi.org/10.1093/molbev/msn218>.

73. Ghalambor, C.K., Walker, J.A., and Reznick, D.N. (2003). Multi-trait Selection, Adaptation, and Constraints on the Evolution of Burst Swimming Performance. *Integr. Comp. Biol.* 43, 431–438. <https://doi.org/10.1093/icb/43.3.431>.

74. Arnold, S.J. (1983). Morphology, performance and fitness. *Am. Zool.* 23, 347–361. <https://doi.org/10.1093/icb/23.2.347>.

75. Irschick, D.J., Meyers, J.J., Husak, J.F., and Le Gilliard, J.-F. (2008). How does selection operate on whole-organism functional performance capacities? A review and synthesis. *Evol. Ecol. Res.* 10, 177–196.

76. Perry, B.W., McGowan, K.L., Arias-Rodriguez, L., Duttke, S.H., Tobler, M., and Kelley, J.L. (2024). Nascent transcription reveals regulatory changes in extremophile fishes inhabiting hydrogen sulfide-rich environments. *Proc. Biol. Sci.* 291, 20240412. <https://doi.org/10.1098/rspb.2024.0412>.

77. Hebert, F.O., Renaut, S., and Bernatchez, L. (2013). Targeted sequence capture and resequencing implies a predominant role of regulatory regions in the divergence of a sympatric lake whitefish species pair (*Coregonus clupeaformis*). *Mol. Ecol.* 22, 4896–4914. <https://doi.org/10.1111/mec.12447>.

78. Seehausen, O., Butlin, R.K., Keller, I., Wagner, C.E., Boughman, J.W., Hohenlohe, P.A., Peichel, C.L., Saetre, G.P., Bank, C., Bränström, A., et al. (2014). Genomics and the origin of species. *Nat. Rev. Genet.* 15, 176–192. <https://doi.org/10.1038/nrg3644>.

79. Ishikawa, A., Kusakabe, M., Yoshida, K., Ravinet, M., Makino, T., Toyoda, A., Fujiyama, A., and Kitano, J. (2017). Different contributions of local- and distant-regulatory changes to transcriptome divergence between stickleback ecotypes. *Evolution* 71, 565–581. <https://doi.org/10.1111/evo.13175>.

80. Kautt, A.F., Kratochwil, C.F., Nater, A., Machado-Schiaffino, G., Olave, M., Henning, F., Torres-Dowdall, J., Häger, A., Hulsey, C.D., Franchini, P., et al. (2020). Contrasting signatures of genomic divergence during sympatric speciation. *Nature* 588, 106–111. <https://doi.org/10.1038/s41586-020-2845-0>.

81. Flaxman, S.M., Wacholder, A.C., Feder, J.L., and Nosil, P. (2014). Theoretical models of the influence of genomic architecture on the dynamics of speciation. *Mol. Ecol.* 23, 4074–4088. <https://doi.org/10.1111/mec.12750>.

82. Renaut, S., Grassa, C.J., Yeaman, S., Moyers, B.T., Lai, Z., Kane, N.C., Bowers, J.E., Burke, J.M., and Rieseberg, L.H. (2013). Genomic islands of divergence are not affected by geography of speciation in sunflowers. *Nat. Commun.* 4, 1827. <https://doi.org/10.1038/ncomms2833>.

83. Han, F., Lamichhaney, S., Grant, B.R., Grant, P.R., Andersson, L., and Webster, M.T. (2017). Gene flow, ancient polymorphism, and ecological adaptation shape the genomic landscape of divergence among Darwin's finches. *Genome Res.* 27, 1004–1015. <https://doi.org/10.1101/gr.212522.116>.

84. Feder, J.L., Nosil, P., Wacholder, A.C., Egan, S.P., Berlocher, S.H., and Flaxman, S.M. (2014). Genome-wide congealing and rapid transitions across the speciation continuum during speciation with gene flow. *J. Hered.* 105, 810–820. <https://doi.org/10.1093/jhered/esu038>.

85. Greenway, R., De-Kayne, R., Brown, A., Camarillo, H., Delich, C., McGowan, K., Nelson, J., Arias-Rodrguez, L., Kelley, J., and Tobler, M. (2024). Integrative analyses of convergent adaptation in sympatric extremophile fishes. Preprint at bioRxiv. <https://doi.org/10.1101/2021.06.28.450104>.

86. Schartl, M., Walter, R.B., Shen, Y., Garcia, T., Catchen, J., Amores, A., Braasch, I., Chalopin, D., Wolff, J.-N., Lesch, K.-P., et al. (2013). The genome of the platyfish, *Xiphophorus maculatus*, provides insights into evolutionary adaptation and several complex traits. *Nat. Genet.* 45, 567–572. <https://doi.org/10.1038/ng.2604>.

87. Setiamarga, D.H.E., Miya, M., Yamanoue, Y., Mabuchi, K., Satoh, T.P., Inoue, J.G., and Nishida, M. (2008). Interrelationships of Atherinomorpha (medakas, flyingfishes, killifishes, silversides, and their relatives): The first evidence based on whole mitogenome sequences. *Mol. Phylogenet. Evol.* 49, 598–605. <https://doi.org/10.1016/j.ympev.2008.08.008>.

88. Rohlf, F.J. (2004). *tpsDig*. <http://life.bio.sunysb.edu/morph/>.

89. Robinson, M.D., McCarthy, D.J., and Smyth, G.K. (2010). edgeR: a Bioconductor package for differential expression analysis of digital gene expression data. *Bioinformatics* 26, 139–140. <https://doi.org/10.1093/bioinformatics/btp616>.

90. Adams, D.C., Collyer, M.L., Kallontzopoulou, A., and Balken, E.K. (2021). Geomorph: Software for geometric morphometric analyses. <https://rune.une.edu.au/web/handle/1959.11/21330>.

91. Warnes, G.R., Bolker, B., Bonebakker, L., Gentleman, R., Huber, W., Liaw, A., Lumley, T., Maechler, M., Magnusson, A., Moeller, S., et al. (2009). gplots: various R programming tools for plotting data. <https://cran.r-project.org/web/packages/gplots/index.html>.

92. Bates, D., Mächler, M., Bolker, B., and Walker, S. (2015). Fitting linear mixed-effects models using lme4. *J. Stat. Softw.* 67, 1–48. <https://doi.org/10.18637/jss.v067.i01>.

93. Therneau, T. (2024). A package for survival analysis in R. <https://cran.r-project.org/web/packages/survival/vignettes/survival.pdf>.
94. Kassambara, A., Kosinski, M., and Biecek, P. (2021). survminer: drawing survival curves using "ggplot2". <https://cran.r-project.org/web/packages/survminer/survminer.pdf>.
95. Krueger, F. (2014). Trim Galore!. https://github.com/felixkrueger/trim_galore.
96. Li, H., and Durbin, R. (2009). Fast and accurate short read alignment with Burrows-Wheeler transform. *Bioinformatics* 25, 1754–1760. <https://doi.org/10.1093/bioinformatics/btp324>.
97. Imelfort, M. (2012). GFF2FASTA. <https://github.com/minillim/gff2fasta>.
98. Pertea, M., Pertea, G.M., Antonescu, C.M., Chang, T.-C., Mendell, J.T., and Salzberg, S.L. (2015). StringTie enables improved reconstruction of a transcriptome from RNA-seq reads. *Nat. Biotechnol.* 33, 290–295. <https://doi.org/10.1038/nbt.3122>.
99. Pertea, M., Kim, D., Pertea, G.M., Leek, J.T., and Salzberg, S.L. (2016). Transcript-level expression analysis of RNA-seq experiments with HISAT, StringTie and Ballgown. *Nat. Protoc.* 11, 1650–1667. <https://doi.org/10.1038/nprot.2016.095>.
100. Eden, E., Navon, R., Steinfeld, I., Lipson, D., and Yakhini, Z. (2009). GOrilla: a tool for discovery and visualization of enriched GO terms in ranked gene lists. *BMC Bioinformatics* 10, 48. <https://doi.org/10.1186/1471-2105-10-48>.
101. McKenna, A., Hanna, M., Banks, E., Sivachenko, A., Cibulskis, K., Kernytsky, A., Garimella, K., Altshuler, D., Gabriel, S., Daly, M., et al. (2010). The Genome Analysis Toolkit: a MapReduce framework for analyzing next-generation DNA sequencing data. *Genome Res.* 20, 1297–1303. <https://doi.org/10.1101/gr.107524.110>.
102. Broad Institute (2018). Picard Toolkit. <https://broadinstitute.github.io/picard/>.
103. Danecek, P., Auton, A., Abecasis, G., Albers, C.A., Banks, E., DePristo, M.A., Handsaker, R.E., Lunter, G., Marth, G.T., Sherry, S.T., et al. (2011). The variant call format and VCFtools. *Bioinformatics* 27, 2156–2158. <https://doi.org/10.1093/bioinformatics/btr330>.
104. Raj, A., Stephens, M., and Pritchard, J.K. (2014). fastSTRUCTURE: variational inference of population structure in large SNP data sets. *Genetics* 197, 573–589. <https://doi.org/10.1534/genetics.114.164350>.
105. Chang, C.C., Chow, C.C., Tellier, L.C., Vattikuti, S., Purcell, S.M., and Lee, J.J. (2015). Second-generation PLINK: rising to the challenge of larger and richer datasets. *Gigascience* 4, 7. <https://doi.org/10.1186/s13742-015-0047-8>.
106. Dierckxsens, N., Mardulyn, P., and Smits, G. (2017). NOVOPlasty: de novo assembly of organelle genomes from whole genome data. *Nucleic Acids Res.* 45, e18. <https://doi.org/10.1093/nar/gkw955>.
107. Iwasaki, W., Fukunaga, T., Isagozawa, R., Yamada, K., Maeda, Y., Satoh, T.P., Sado, T., Mabuchi, K., Takeshima, H., Miya, M., et al. (2013). MitoFish and MitoAnnotator: a mitochondrial genome database of fish with an accurate and automatic annotation pipeline. *Mol. Biol. Evol.* 30, 2531–2540. <https://doi.org/10.1093/molbev/mst141>.
108. Katoh, K., Kuma, K.-I., Toh, H., and Miyata, T. (2005). MAFFT version 5: improvement in accuracy of multiple sequence alignment. *Nucleic Acids Res.* 33, 511–518. <https://doi.org/10.1093/nar/gki198>.
109. Abascal, F., Zardoya, R., and Telford, M.J. (2010). TranslatorX: multiple alignment of nucleotide sequences guided by amino acid translations. *Nucleic Acids Res.* 38, W7–W13. <https://doi.org/10.1093/nar/gkq291>.
110. Leigh, J.W., and Bryant, D. (2015). Popart: Full-feature software for haplotype network construction. *Methods Ecol. Evol.* 6, 1110–1116. <https://doi.org/10.1111/2041-210X.12410>.
111. Felsenstein, J. (1989). PHYLIP - Phylogeny Inference Package (Version 3.2). *Cladistics* 5, 164–166.
112. Yang, Z. (2007). PAML 4: Phylogenetic analysis by maximum likelihood. *Mol. Biol. Evol.* 24, 1586–1591. <https://doi.org/10.1093/molbev/msm088>.
113. Quinlan, A.R., and Hall, I.M. (2010). BEDTools: a flexible suite of utilities for comparing genomic features. *Bioinformatics* 26, 841–842. <https://doi.org/10.1093/bioinformatics/btq033>.
114. Greenway, R., Arias-Rodriguez, L., Diaz, P., and Tobler, M. (2014). Patterns of macroinvertebrate and fish diversity in freshwater sulphide springs. *Diversity* 6, 597–632. <https://doi.org/10.3390/d6030597>.
115. Palacios, M., Arias-Rodriguez, L., Plath, M., Eifert, C., Lerp, H., Lamboj, A., Voelker, G., and Tobler, M. (2013). The rediscovery of a long described species reveals additional complexity in speciation patterns of poeciliid fishes in sulfide springs. *PLoS One* 8, e71069. <https://doi.org/10.1371/journal.pone.0071069>.
116. Álvarez del Villar, J. (1948). Descripción de una nueva especie de *Mollieenisia* capturada en Baños del Azufre, Tabasco (Pisces Poeciliidae). *An. Esc. Nac. Cienc. Biol.* 5, 275–281.
117. Butler, I.B., Schoonen, M.A.A., and Rickard, D.T. (1994). Removal of dissolved oxygen from water: a comparison of four common techniques. *Talanta* 41, 211–215. [https://doi.org/10.1016/0039-9140\(94\)80110-x](https://doi.org/10.1016/0039-9140(94)80110-x).
118. Evans, D.H., and Claiborne, J.B. (2006). *The Physiology of Fishes* (Taylor & Francis).
119. Tobler, M., Riesch, R., Tobler, C.M., Schulz-Mirbach, T., and Plath, M. (2009). Natural and sexual selection against immigrants maintains differentiation among micro-allopatric populations. *J. Evol. Biol.* 22, 2298–2304. <https://doi.org/10.1111/j.1420-9101.2009.01844.x>.
120. Zelditch, M.L., Swiderski, D.L., and David Sheets, H. (2012). *Geometric Morphometrics for Biologists: A Primer* (Academic Press).
121. Langerhans, R.B. (2009). Trade-off between steady and unsteady swimming underlies predator-driven divergence in *Gambusia affinis*. *J. Evol. Biol.* 22, 1057–1075. <https://doi.org/10.1111/j.1420-9101.2009.01716.x>.
122. Klingenberg, C.P., and Spence, J.R. (1993). Heterochrony and allometry: lessons from the water strider genus *Limnoporus*. *Evolution* 47, 1834–1853. <https://doi.org/10.1111/j.1558-5646.1993.tb01273.x>.
123. Therneau, T., and Grambsch, P. (2001). *Modeling Survival Data: Extending the Cox Model*, First Edition (Springer).
124. Camacho, C., Coulouris, G., Avagyan, V., Ma, N., Papadopoulos, J., Bealer, K., and Madden, T.L. (2009). BLAST+: architecture and applications. *BMC Bioinformatics* 10, 421. <https://doi.org/10.1186/1471-2105-10-421>.
125. Benjamini, Y., and Hochberg, Y. (1995). Controlling the false discovery rate: A practical and powerful approach to multiple testing. *J. R. Stat. Soc. Series B Stat. Methodol.* 57, 289–300. <https://doi.org/10.1111/j.2517-6161.1995.tb02031.x>.
126. Harris, M.A., Clark, J., Ireland, A., Lomax, J., Ashburner, M., Foulger, R., Eilbeck, K., Lewis, S., Marshall, B., Mungall, C., et al. (2004). The Gene Ontology (GO) database and informatics resource. *Nucleic Acids Res.* 32, D258–D261. <https://doi.org/10.1093/nar/gkh036>.
127. DePristo, M.A., Banks, E., Poplin, R., Garimella, K.V., Maguire, J.R., Hartl, C., Philippakis, A.A., del Angel, G., Rivas, M.A., Hanna, M., et al. (2011). A framework for variation discovery and genotyping using next-generation DNA sequencing data. *Nat. Genet.* 43, 491–498. <https://doi.org/10.1038/ng.806>.
128. Van der Auwera, G.A., Carneiro, M.O., Hartl, C., Poplin, R., Del Angel, G., Levy-Moonshine, A., Jordan, T., Shakir, K., Roazen, D., Thibault, J., et al. (2013). From FastQ data to high confidence variant calls: the Genome Analysis Toolkit best practices pipeline. *Curr. Protoc. Bioinformatics* 43, 11.10.1–11.10.33. <https://doi.org/10.1002/0471250953.bi110s43>.
129. Korunes, K.L., and Samuk, K. (2021). pixy: Unbiased estimation of nucleotide diversity and divergence in the presence of missing data. *Mol. Ecol. Resour.* 21, 1359–1368. <https://doi.org/10.1111/1755-0998.13326>.
130. Gutenkunst, R.N., Hernandez, R.D., Williamson, S.H., and Bustamante, C.D. (2009). Inferring the joint demographic history of multiple populations from multidimensional SNP frequency data. *PLoS Genet.* 5, e1000695. <https://doi.org/10.1371/journal.pgen.1000695>.
131. Recknagel, H., Elmer, K.R., and Meyer, A. (2013). A hybrid genetic linkage map of two ecologically and morphologically divergent *Midas*

cichlid fishes (*Amphilophus* spp.) obtained by massively parallel DNA sequencing (ddRADSeq). *G3 (Bethesda)* 3, 65–74. <https://doi.org/10.1534/g3.112.003897>.

132. Jourdan, J., Bierbach, D., Riesch, R., Schießl, A., Wigh, A., Arias-Rodriguez, L., Indy, J.R., Klaus, S., Zimmer, C., and Plath, M. (2014). Microhabitat use, population densities, and size distributions of sulfur cave-dwelling *Poecilia mexicana*. *PeerJ* 2, e490. <https://doi.org/10.7717/peerj.490>.

133. Riesch, R., Plath, M., Schlupp, I., Tobler, M., and Brian Langerhans, R.B. (2014). Colonization of toxic environments drives predictable life-history shift in livebearing fishes (Poeciliidae). *Ecol. Lett.* 17, 65–71. <https://doi.org/10.1111/ele.12209>.

134. Clement, M., Snell, Q., Walke, P., Posada, D., and Crandall, K. (2002). TCS: estimating gene genealogies. In Proceedings of the 16th International Parallel and Distributed Processing Symposium (IEEE). <https://doi.org/10.1109/IPDPS.2002.1016585>.

135. Li, H., Handsaker, B., Wysoker, A., Fennell, T., Ruan, J., Homer, N., Marth, G., Abecasis, G., and Durbin, R.; 1000 Genome Project Data Processing Subgroup (2009). The Sequence Alignment/Map format and SAMtools. *Bioinformatics* 25, 2078–2079. <https://doi.org/10.1093/bioinformatics/btp352>.

136. Zhang, J., Nielsen, R., and Yang, Z. (2005). Evaluation of an improved branch-site likelihood method for detecting positive selection at the molecular level. *Mol. Biol. Evol.* 22, 2472–2479. <https://doi.org/10.1093/molbev/msi237>.

137. Martin, S.H., Davey, J.W., and Jiggins, C.D. (2015). Evaluating the use of ABBA-BABA statistics to locate introgressed loci. *Mol. Biol. Evol.* 32, 244–257. <https://doi.org/10.1093/molbev/msu269>.

138. Martin, S.H., Singh, K.S., Gordon, I.J., Omufwoko, K.S., Collins, S., Warren, I.A., Munby, H., Brattström, O., Traut, W., Martins, D.J., et al. (2020). Whole-chromosome hitchhiking driven by a male-killing endosymbiont. *PLoS Biol.* 18, e3000610. <https://doi.org/10.1371/journal.pbio.3000610>.

139. Martin, S. (2020). General tools for genomic analyses (GitHub). https://github.com/simonhmartin/genomics_general.

140. Delmore, K.E., Lugo Ramos, J.S., Van Doren, B.M., Lundberg, M., Bensch, S., Irwin, D.E., and Liedvogel, M. (2018). Comparative analysis examining patterns of genomic differentiation across multiple episodes of population divergence in birds. *Evol. Lett.* 2, 76–87. <https://doi.org/10.1002/evl3.46>.

STAR★METHODS

KEY RESOURCES TABLE

REAGENT or RESOURCE	SOURCE	IDENTIFIER
Biological samples		
Tissue samples preserved in RNAlater	This paper	N/A
Chemicals, peptides, and recombinant proteins		
High Sensitivity NGS Fragment Analysis Kit	Agilent	DNF-474-0500
TruSeq Nano DNA Library Prep Kit	Illumina	20015965
HiSeq Cluster Kit v4	Illumina	PE-401-4001
HiSeq SBS kit v4	Illumina	FC-401-4001
RNAlater Stabilizing Solution	Invitrogen	CAS 7783-20-2
KAPA Library Quantification Kit	KAPA Biosystems	KR0405 – v11.20
NucleoSpin RNA Kit	Macherey-Nagel	REF 740955.50
NucleoSpin Tissue Kit	Macherey-Nagel	REF 740952.50
NEBNext Poly(A) mRNA Magnetic Isolation Module	New England Biolabs	NEB #E7490
NEBNext Ultra Directional RNA Library Prep Kit for Illumina	New England Biolabs	NEB #E7420
Sodium sulfide hydrate (Na ₂ S·6H ₂ O)	Sigma	CAS 27610-45-3
Tris hydrochloride (Tris HCl)	Sigma	CAS 1185-53-1
Sodium hydroxide (NaOH)	Sigma	CAS 1310-73-2
Qubit dsDNA Quantification Assay Kits	Thermo Fisher Scientific	Q32851
Deposited data		
<i>X. maculatus</i> reference genome	Schartl et al. ^{18,86}	GenBank assembly: GCF_002775205.1
<i>X. maculatus</i> mitochondrial genome	Setiamarga et al. ^{85,87}	GenBank assembly: NC_011379
RNA sequences of <i>P. bimaculatus</i> and <i>X. hellerii</i>	This study, Greenway et al. ²⁶	NCBI BioProject: PRJNA608180
RNA sequences of <i>P. mexicana</i> ,	This study	NCBI BioProject: PRJNA1152527
DNA sequences of <i>P. mexicana</i> , <i>P. bimaculatus</i> , and <i>X. hellerii</i>	This study	NCBI BioProject: PRJNA738871
Data on water quality, body shape, H ₂ S tolerance, and survival in translocation experiments	This study	Dryad, https://doi.org/10.5061/dryad.pg4f4qrzv
Software and algorithms		
tpsDig	Rohlf ⁸⁸	https://www.sbmorphometrics.org/soft-dataacq.html
edgeR (R package)	Robinson et al. ⁸⁹	https://bioconductor.org/packages/release/bioc/html/edgeR.html
GEOMORPH (R package)	Adams et al. ⁹⁰	https://cran.r-project.org/web/packages/geomorph/index.html
GPLOTS (R package)	Warnes et al. ⁹¹	https://cran.r-project.org/web/packages/gplots/index.html
LME4 (R package)	Bates et al. ⁹²	https://cran.r-project.org/web/packages/lme4/index.html
MINOTAUR (R package)	Verity et al. ⁴⁰	https://github.com/NESCent/MINOTAUR
SURVIVAL (R package)	Therneau ⁹³	https://cran.r-project.org/web/packages/survival/index.html
SURVMINER (R package)	Kassambara et al. ⁹⁴	https://cran.r-project.org/web/packages/survminer/index.html

(Continued on next page)

Continued

REAGENT or RESOURCE	SOURCE	IDENTIFIER
TrimGalore!	Kruger ⁹⁵	https://github.com/FelixKrueger/TrimGalore
BWA-MEM	Li and Durbin ⁹⁶	https://github.com/lh3/bwa
gff2fasta.pl	Imelfort ⁹⁷	https://github.com/minillinim/gff2fasta
StringTie	Pertea et al. ^{98,99}	https://ccb.jhu.edu/software/stringtie/
GORilla	Eden et al. ¹⁰⁰	https://cbl-gorilla.cs.technion.ac.il/
bcl2fastq2.17.1.14	Hepler	https://github.com/thepler/bcl2fastq2
Genome Analysis Toolkit	McKenna et al. ¹⁰¹	https://gatk.broadinstitute.org/
Picard Tools	Broad Institute ¹⁰²	https://broadinstitute.github.io/picard/
VCFtools	Danecek et al. ¹⁰³	https://vcftools.sourceforge.net/
FastStructure	Raj et al. ¹⁰⁴	https://rajanil.github.io/fastStructure/
PLINK	Chang et al. ¹⁰⁵	https://www.cog-genomics.org/plink/2.0/
NOVOPlasty	Dierckxsens et al. ¹⁰⁶	https://github.com/ndierckx/NOVOPlasty
MitoAnnotator	Iwasaki et al. ¹⁰⁷	https://mitofish.aori.u-tokyo.ac.jp/annotation/input/
MAFFT	Katoh et al. ¹⁰⁸	https://mafft.cbrc.jp/alignment/software/
TranslatorX	Abascal et al. ¹⁰⁹	http://translatorx.co.uk
PopART	Leigh and Bryant ¹¹⁰	https://github.com/jessicawleigh/popart
PHYLIP	Felsenstein ¹¹¹	https://phylipweb.github.io/phylip/
PAML	Yang ¹¹²	http://abacus.gene.ucl.ac.uk/software/paml.html
BEDTools	Quinlan and Hall ¹¹³	https://bedtools.readthedocs.io/en/latest/

EXPERIMENTAL MODEL AND SUBJECT DETAILS

In the foothills of the Sierra Madre de Chiapas, several freshwater springs rich in naturally occurring H₂S form the La Gloria spring complex.^{43,114} The spring complex is located near the city of Teapa, Mexico, and is part of the Río Pichucalco drainage. Habitats with high H₂S concentrations are spatially restricted (~200 m in length), and the spring run flows directly into a nearby nonsulfidic stream (Arroyo Caracol). There are no physical barriers that prevent fish movement between the sulfidic spring run and the nonsulfidic stream, but there are stark differences in water chemistry (Figure 1). Populations of the poeciliid fishes *Poecilia mexicana*, *Pseudoxiphophorus bimaculatus*, and *Xiphophorus hellerii* have colonized H₂S-rich habitats at La Gloria, and ancestral populations also occur in adjacent nonsulfidic habitats.¹¹⁵ Note that the population of *P. mexicana* at La Gloria likely belongs to an endemic species described from sulfide springs, *P. sulphuraria*.^{115,116} All samples used in this study were collected by seine from the La Gloria sulfide spring complex and nonsulfidic habitats in the adjacent Arroyo Caracol. The sole exception were *Pseudoxiphophorus* gill tissues for the nonsulfidic population, which were collected from another nearby stream (Table S5).

METHOD DETAILS**Water chemistry**

Physical and chemical water parameters were analyzed for several sites within the La Gloria spring complex and Arroyo Caracol. Temperature, specific conductivity, pH, and oxygen content were measured using a Hydrolab Multisonde 4A (Hach Environmental). Environmental H₂S concentrations were measured with a methylene blue assay using a Hach DR1900 Portable Spectrophotometer (Hach Company, Loveland, CO, USA). Measurements and calibration of probes were conducted according to the manufacturer's recommendations. At least three Hydrolab readings and two H₂S samples were taken at each site. Measurements were averaged for each site prior to use in a principal component analysis.

Body shape

To test for divergence in body shape among populations in sulfidic and nonsulfidic habitats, adult *Poecilia*, *Pseudoxiphophorus*, and *Xiphophorus* were collected from the two sites using seines. Lateral photographs were taken for all specimens using a Canon EOS 400D digital camera (Canon USA Inc., Lake Success, NY, USA) mounted on a copy stand. We digitized 14 morphological landmarks (Figure S6) on each photograph using the software program tpsDig.⁸⁸

Tolerance to acute H₂S exposure

To test for differences in H₂S tolerance between individuals collected from the sulfidic and nonsulfidic populations, we conducted acute H₂S exposure trials, subjecting wild-caught fish to logarithmically increasing concentrations of H₂S.⁴³ We collected adult

Poecilia, *Pseudoxiphophorus*, and *Xiphophorus* from the two sites using seines, transferred them to insulated coolers filled with water from the collection site, and transported them to a nearby field station. Fish were kept in population and species-specific holding tanks with aeration for at least 24 hours prior to testing. To standardize experimental conditions, water from the collection sites was slowly replaced with H₂S-free well water over the first 8 hours in the holding tanks. Water was continuously aerated and filtered during this time, and the fish received no food.

For the experiment, we prepared stock solutions of 10 mM aqueous H₂S solution by dissolving 2.4 g sodium sulfide hydrate (Na₂S·6H₂O) into 1 L of well water deoxygenated through purging with nitrogen gas.¹¹⁷ Individual fish were placed into clear plastic containers with 150 mL water from the holding tanks and allowed to acclimate for 5 minutes. Following acclimation, 10 mL of H₂S solution were added to the experimental container at 2-minute intervals using a syringe placed under the water surface. Each fish was observed as H₂S concentration increased in the experimental container. We measured the time until the fish lost equilibrium, at which point the fish was removed from the container, sexed, weighed, and placed into a heavily aerated recovery tank. Experiments were ended after 32 minutes (15 sulfide additions) if a fish did not lose equilibrium.

Gene expression variation

We used an RNA-sequencing approach to identify differentially expressed genes between the sulfidic and nonsulfidic populations of each species. We collected adult female individuals of *Poecilia*, *Pseudoxiphophorus*, and *Xiphophorus* in the La Gloria sulfide spring and from the adjacent nonsulfidic stream. Following capture with a seine, fish were instantly euthanized, and gill tissues were extracted from both sides of the head and immediately preserved in 2 mL of RNAlater (Invitrogen, Inc.). We selected gill tissue because the gills mediate physiological processes necessary for the maintenance of homeostasis,¹¹⁸ are in direct contact with the H₂S-rich water,¹⁶ and show strong, heritable transcriptional responses upon H₂S exposure.^{31,48} RNA was isolated from gill tissues, and cDNA libraries were constructed for each sample as described for samples in previous studies.^{26,48} We extracted total RNA from pulverized gill tissues using the NucleoSpin RNA kit (Macherey-Nagel GmbH & Co. KG, Düren, Germany) following the manufacturer's protocol. We conducted mRNA isolation and cDNA library preparation with the NEBNext Poly(A) mRNA Magnetic Isolation Module (New England Biolabs, Inc., Ipswich, MA, USA) and NEBNext Ultra Directional RNA Library Prep Kit for Illumina (New England Biolabs, Inc., Ipswich, MA, USA), following the manufacturers' protocol with minor modifications. Each cDNA library was assigned a unique barcode, quantified, and pooled in sets of 11–12 samples that were sequenced together in a way that different species and habitat types were sequenced together. cDNA libraries were sequenced on an Illumina HiSeq 2500 with paired-end, 100-bp reads at the Washington State University Spokane Genomics Core.

Genome sequencing

We resequenced the genomes of 120 individuals (40 per species, 20 per population). DNA was extracted from fin clip tissues that were stored in ethanol using the NucleoSpin Tissue kit (Macherey-Nagel GmbH & Co. KG, Düren, Germany) following the protocol in the user manual (version January 2017/Rev. 17). For the final elution step, extracted DNA was eluted in 100 μL of elution buffer.

Library preparation and sequencing were conducted at the Washington State University Spokane Genomics Core. Genomic DNA (gDNA) was quantified using the Qubit 2.0 fluorometer with the dsDNA HS assay kit (Thermo Fisher Scientific, Waltham, MA). One hundred nanograms of gDNA were used as input for library preparation using the TruSeq Nano DNA Library Prep Kit (Illumina, San Diego, CA). gDNA was sheared using the M220 Focused-Ultrasonicater (Covaris, Woburn, MA), followed by end repair, size selection (350-bp insert size), dA-tailing, adaptor ligation, and library amplification by eight rounds of PCR. The quality of the DNA libraries was assessed by Fragment Analyzer with the High Sensitivity NGS Fragment Analysis Kit (Advanced Analytical Technologies, Ankeny, IA). Library concentrations were measured by the StepOnePlus Real-Time PCR System (ThermoFisher Scientific, Waltham, MA) with the KAPA Library Quantification Kit (KAPA Biosystems, Wilmington, MA). Each library was labeled with an index sequence during the adaptor-ligation step using Illumina's TruSeq Dual Indexing system (Illumina, San Diego, CA), which contains 96 unique indices. The 120 libraries were split and pooled into two groups at equal molar concentrations, with each library having a unique index within its group. The library pools were diluted to 2 nM with Reticulocyte Standard Buffer (RSB; 10 mM Tris-HCl, pH 8.5) and denatured with 0.1 M NaOH. Eighteen pM libraries were clustered in a high-output flow cell using the HiSeq Cluster Kit v4 on a cBot (Illumina, San Diego, CA). After cluster generation, the flow cell was loaded onto HiSeq 2500 for sequencing using the HiSeq SBS kit v4 (Illumina, San Diego, CA). DNA was sequenced with paired-end, 100-bp chemistry among four lanes. Raw bcl files were converted to fastq files and demultiplexed using the program bcl2fastq2.17.1.14 (<https://github.com/thepler/bcl2fastq2>).

Reciprocal translocation experiment

To experimentally validate local adaptation³³ and test for natural selection against migrants between sulfidic and nonsulfidic populations,³⁴ we conducted reciprocal translocation experiments using previously established approaches.^{20,119} Large (20-liter) plastic buckets were placed into the two habitat types as experimental mesocosms. Two holes (18 × 32 cm) were cut into opposite sides of each bucket and sealed with 1.5 mm plastic mesh to allow the free exchange of water with the environment. Approximately 50 small holes (<1 mm) were drilled into the bucket lids to facilitate air exchange. Mesocosms were placed into shallow areas of the sulfidic and nonsulfidic streams, seeded with a 3–4 cm layer of natural substrate, and allowed to settle overnight before the start of the experiment. We established ten mesocosms in each habitat. Water conditions in these mesocosms have been shown to closely match conditions in the surrounding stream.¹¹⁹

We collected adult *Poecilia*, *Pseudoxiphophorus*, and *Xiphophorus* by seine and placed them in insulated coolers with aerated water for transport to the mesocosm locations. Five haphazardly chosen individuals of the same species and habitat type were introduced into a mesocosm. Half of the mesocosms in each habitat were used as controls to test the survival of resident fish, and the other half to test survival of fish from the opposite habitat type. Transportation and handling times were minimal (<1 hour) and were balanced for resident and translocated individuals. Fish were measured for standard length prior to introduction. Experiments ran for ~20 hours before termination. Following the experimental period, we quantified survival and returned surviving individuals to their original collection site.

QUANTIFICATION AND STATISTICAL ANALYSIS

Analysis of body shape

We extracted coordinates of these digitized landmarks to conduct geometric morphometric analyses¹²⁰ using the GEOMORPH package in R.⁹⁰ We first aligned landmark coordinates via least-squares superimposition implemented in the gpagen function to remove effects of translation, rotation, and scale, yielding aligned Procrustes coordinates that describe body shape variation and centroid size as a measure of size. Procrustes coordinates were then analyzed using a Procrustes ANOVA (procD.lm) using residual randomization over 9999 iterations and type III sums of squares. Predictor variables included species (*Poecilia*, *Pseudoxiphophorus*, or *Xiphophorus*), habitat (sulfidic vs. non-sulfidic), and sex as factors, centroid size as a covariate, as well as their interaction terms. *P*-values were based on a Cohen's f-squared sampling distribution. For data visualization, we calculated divergence vector scores¹²¹ for each individual based on the first principle component of the among-group covariance matrix for the habitat term from a preparatory MANCOVA using the same model as for the Procrustes ANOVA.¹²² This approach allowed us to visualize aspects of body shape variation associated with habitat type among species (i.e., convergent aspects of body shape), while accounting for all other terms in the model.

Analysis of tolerance to acute H₂S exposure

We analyzed variation in H₂S tolerance using a survival analysis (Cox regression) with the coxph function implemented in the R package SURVIVAL.^{93,123} We used time to loss of equilibrium as the response variable, and individuals that did not lose equilibrium during the experiment were censored. Body mass (log₁₀-transformed), species, sex, and habitat of origin (sulfidic vs. nonsulfidic) were used as independent variables. Adjusted survival curves were generated for the habitat term of the Cox regression to visualize expected survival curves, using the ggadjustedcurves function from the SURVMINER package.⁹⁴

Analysis of gene expression variation

Raw RNA-sequencing reads were sorted by barcode and trimmed twice (*-quality* 0 to remove adapters, followed by *-quality* 24) with TrimGalore!⁹⁵ Trimmed reads for all 36 individuals were mapped to the *X. maculatus* reference genome (v.5.0, RefSeq accession number: GCF_002775205.1)⁸⁶ using BWA-MEM.⁹⁶ On average, ~97% of reads mapped across all individuals (Table S6). We functionally annotated genes from the *X. maculatus* reference genome by extracting the longest transcript per gene (using the perl script gff2fasta.pl)⁹⁷ and then searching against the human SWISSPROT database (critical E-value 0.001; access date 11/15/2018) using BLASTx.¹²⁴ Each *X. maculatus* gene was annotated with the top BLAST hit based on the top high-scoring segment pair. Annotations were used for analysis of differentially expressed genes as well as for analyses of outlier regions from genomic data (see below).

We used StringTie v.1.3.3b^{98,99} to quantify the number of RNA-seq reads mapped to each gene in the *X. maculatus* reference genome for each individual and used a Python script provided with StringTie (prepDE.py) to generate a read counts matrix.⁹⁹ We then removed genes that did not have at least two counts per million in three or more individuals across all species, resulting in a set of 18,598 genes for analysis of gene expression patterns. We first conducted hierarchical cluster analysis on the full set of retained genes. The hierarchical cluster analysis was performed on log₂-transformed counts-per-million and visualized with the heatmap.2 function in the GPLOTS package in R.⁹¹

To identify differentially expressed genes, we used generalized linear models (GLMs) as implemented in the Bioconductor package edgeR.⁸⁹ We used glmFit to fit a negative binomial GLM to the normalized read counts of each gene based on tagwise dispersion estimates and a design matrix describing the comparison between the sulfidic and nonsulfidic population of each species. We assessed statistical significance with the GLM likelihood-ratio test with a false-discovery rate (FDR) of < 0.05 calculated with the Benjamini-Hochberg correction.¹²⁵ We then intersected the significantly upregulated and downregulated genes from all three species-specific comparisons separately to identify genes with consistent evidence for differential expression among all three species. After identifying the set of genes with differential expression between sulfidic and nonsulfidic populations of each species, and genes with evidence for shared differential expression across all three species-specific analyses (Data S1), we used a Gene Ontology (GO) enrichment analysis to explore the putative biological functions of these candidate sets of genes (Data S2). We first annotated all genes that had a match in the human SWISSPROT database with GO IDs.¹²⁶ In total, 10,817 unique SWISSPROT annotations were associated with a term in the GO database. We then tested for the enrichment of specific GO IDs in these sets of genes with differential expression relative to the full dataset of 18,598 analyzed genes using GOrilla (*P*-value threshold: 0.0001, accessed 04/11/2019).¹⁰⁰

Analysis of genome sequencing

Mapping and genotyping

Raw reads were trimmed to remove adapters with Trimgalore! (*–quality 0*).⁹⁵ Trimmed reads for all 120 individuals were mapped to the *Xiphophorus maculatus* reference genome (v.5.0, RefSeq accession number: GCF_002775205.1)⁸⁶ using BWA-MEM.⁹⁶ We used this reference genome because *X. maculatus* was the only species in the family Poeciliidae with a chromosome-scale genome assembly. On average, ~94% of trimmed reads mapped across all individuals (Table S2). After mapping, based on percent of mapped reads, it became clear that one sample (sample MX16-205) labeled as *Pseudoxiphophorus* from a sulfidic habitat was likely mislabeled, and this sample was excluded from all further analyses. Note that we conducted the same analyses mapping to the *P. mexicana* reference genome, and all results were consistent.

The resequenced genomes generated for this study had an average sequence depth of 3.8 (± 0.4 ; Table S2). We used the Genome Analysis Toolkit (GATK, v.3.5)¹⁰¹ and Picard Tools¹⁰² to mark duplicate reads (using the MarkDuplicates tool) and realign mapped reads around indels (using the RealignerTargetCreator and IndelRealigner tools) following GATK best practices.^{127,128} The resulting realigned bam-file for each individual was used in subsequent analyses. GATK was also used to identify single nucleotide polymorphisms (SNPs) per population. HaplotypeCaller was used to identify genotypes per individual with the *–ERC* GVCF flag.¹⁰¹

Samples were genotyped jointly on a per-species basis using GATK's GenotypeGVCFs tool after combining GVCF files from the sulfidic and nonsulfidic populations using the GATK CombineGVCFs tool. Genotypes were identified using the *–include-non-variant-sites* flag to retain all sites in the initial VCF. We recoded genotypes inferred as phased missing (.) as unphased missing (./.) due to a formatting issue with VCFtools. We used the GATK SelectVariants to extract biallelic SNPs from the original genotyped GVCF files, except for the d_{XY} analysis (see below). For all analyses relying on biallelic SNPs, combined VCF files with both the sulfidic and non-sulfidic populations of each species were filtered to exclude sites with >25% missing data, a minor allele frequency below 5%, and alleles that were fixed for the non-reference allele were removed using VCFtools v.0.1.17¹⁰³ with the following flags: *–max-missing* 0.75, *–remove-filtered-all*, *–maf* 0.05, and *–max-non-ref-af-any* 0.999. After filtering, 1,994,206 biallelic SNPs were retained for *Poecilia*, 5,284,684 for *Pseudoxiphophorus*, and 4,624,801 for *Xiphophorus*. For calculating d_{XY} , only indels and sites with >25% missing data were removed from the merged VCF using VCFtools with the *–remove-indels* and *–max-missing* 0.75 flags, respectively (note that this filtering retained monomorphic sites for accurate estimation of d_{XY}).¹²⁹ This resulted in the retention of 439,564,228 monomorphic and biallelic sites for *Poecilia*, 528,674,992 for *Pseudoxiphophorus*, and 611,098,475 for *Xiphophorus*.

Population structure

We assessed structure between populations in sulfidic and nonsulfidic habitats of each species. To do so, we removed sites with an r^2 above 0.7 within 5 kilobases (kb) within VCFtools (*–geno-r2 –min-r2* 0.7 *–ld-window* 5000), producing a set of unlinked SNPs for each species (62,738 in *Poecilia*, 64,405 in *Pseudoxiphophorus*, and 65,515 in *Xiphophorus*). We investigated the extent of gene flow between populations using FastStructure,¹⁰⁴ a maximum-likelihood-based assignment method that estimates admixture proportions for each individual. FastStructure was run with the number of populations (*K*) set as 2 to test if individuals cluster by habitat of origin (i.e., sulfidic vs. nonsulfidic). Population structure was further examined by principal component analysis (PCA) based on a variance-standardized genetic relationship matrix computed with PLINK v.2.00.¹⁰⁵

From the structure analyses, we identified an admixed individual of *P. mexicana* that was likely an F1 hybrid between the sulfidic and non-sulfidic populations (MX16-023). We also identified another admixed individual in *P. mexicana* that was possibly an F1 or F2 backcross (MX16-121). We removed these admixed individuals from the *Poecilia* SNP sets for downstream analyses.

Demographic histories

We used diffusion-approximations for demographic inference ($\partial\alpha\partial i$)¹³⁰ to reconstruct demographic histories for each of the three population pairs. For the demographic analysis, we further filtered our species vcf files from the jointly genotyped SNP set described in the methods using VCFtools.¹⁰³ Specifically, we only kept sites if they were biallelic (*–max-alleles* 2 and *–min-alleles* 2), present at a depth of at least 6' (*–minDP* 8) in at least 75 % of the individuals (*–max-missing* 0.75), and had a quality score of at least 30 (*–minQ* 30), resulting in 59,588 SNPs for *Poecilia*, 72,327 for *Pseudoxiphophorus*, and 77,117 for *Xiphophorus*. Three general models were compared for each pair: (1) a population split followed by migration (full migration model); (2) a population split followed by a period where migration was allowed, but with migration stopping at some point in time (ancient migration model); and (3) a population split followed by a period without migration, but with migration starting at some point later in time (secondary contact model). To fully explore the parameter space, we started each model from 20 different, randomly selected points in the parameter space, and we performed additional runs of each model where we restricted migration in one or both directions. Singletons were masked to reduce potential effects of sequencing errors on the models. We also downsampled to 24 chromosomes per population to account for missing genotypes. Akaike Information Criterion with small-sample correction (AICc) was used to compare the fit of the models. We assumed a mutation rate of 6.6×10^{-8} mutations per site per generation¹³¹ and a generation time of six months^{132,133} to convert $\partial\alpha\partial i$ parameters to effective population sizes, migration rates per generation, and timing of events (i.e., divergence times or times when migratory patterns changed). We performed 100 bootstrap replicates of the best model for each population pair to obtain 95 % confidence intervals for all parameters. To ascertain that results were not biased by SNPs in regions of the genome under selection or by recent gene flow, we ran additional models excluding admixed individuals and with only putatively neutral SNPs as input. To obtain a set of putatively neutral SNPs, we filtered out all SNPs found within gene regions in the genome annotation (GTF) file using the intersect tool within BEDTools v.2.25.0.¹¹³ We removed the apparent F1 individual from the sulfidic *Poecilia* population to limit its

effect on our demographic models using the `–remove-indv` option within VCFtools v.0.1.15.¹⁰³ Models run with this set of SNPs recovered quantitatively similar results, with overlapping confidence intervals to model parameters estimated with SNPs from all regions of the genome.

Mitochondrial genome assembly and analysis

Trimmed reads from the whole-genome re-sequencing were used as input for NOVOPlasty,¹⁰⁶ which allows for *de novo* assembly and variant-calling in short circular genomes. The *X. maculatus* reference mitochondrial genome (NCBI Accession NC_011379⁸⁷) was used as the seed input and reference sequence. Sequences for the 13 protein-coding genes were identified using MitoAnnotator.¹⁰⁷

To investigate the evolutionary history of mitochondrial genomes among populations, we performed phylogenetic analyses using 12 of the 13 protein-coding mitochondrial genes (*atp8* was excluded from analyses due to poor assembly for this short gene in many individuals). For each gene, we aligned nucleotide sequences of all individuals using the default options of the MAFFT progressive alignment method,¹⁰⁸ guided by a translated amino acid sequence with TranslatorX.¹⁰⁹ We used PopART v.1.7¹¹⁰ to construct a TCS haplotype network¹³⁴ for the concatenated mitochondrial sequences of each population pair separately.

Since mitochondria and OxPhos are the direct target of H₂S toxicity, we analyzed patterns of molecular evolution and the effect of positive selection in lineages from sulfidic habitats for 12 of the 13 mitochondrial encoded protein-coding genes, following a previously developed approach.²⁶ In brief, because of the high coverage of the RNAseq data, we used GATK¹⁰¹ to realign BWA-MEM mapped RNAseq reads around indels and used the UnifiedGenotyper to detect variants following GATK best practices.^{127,128} We genotyped individuals on a per-population basis using the UnifiedGenotyper EMIT_ALL_SITES output mode to create a VCF-file for each population. We then used a custom pipeline to fill positions lacking sequence data in each VCF with Ns, rather than the GATK default (which fills in missing data with the reference allele).¹³⁵ We used VCFtools v.1.3 to designate the genotype at all variable sites as the major allele in each population's VCF-file with the setGT tool.¹⁰³ Using the coordinates for each mitochondrial gene from the *X. maculatus* reference genome gene annotation file (GTF), we created population-specific consensus sequences for each mitochondrial gene across all individuals in a population using the consensus tool in BCFtools. We aligned nucleotide sequences for all populations using the MAFFT progressive alignment method¹⁰⁸ guided by the translated amino acid sequence as implemented in TranslatorX,¹⁰⁹ producing an in-frame multispecies alignment of each gene. We constructed gene-specific phylogenies (gene trees) for each sequence using the DNAML program in PHYLP v.3.696.¹¹¹

To identify mitochondrial genes that have experienced positive selection in multiple sulfide spring populations, as evidenced by an excess rate of non-synonymous to synonymous substitutions (ω) for codons in each mitochondrial gene across the sulfidic branches of our phylogenies, we used branch models implemented by codeml in PAML v.4.9a.¹¹² For each mitochondrial gene, codeml was run using the in-frame multispecies alignment and gene tree with the three sulfidic populations designated as foreground branches and nonsulfidic populations as background branches, allowing us to test whether ω differed between foreground and background branches in a two-ratio branch model (M2; model = 2, NSsites = 0) compared against a null model with a single ω value for all branches (M0; model = 0, NSsites = 0). A likelihood-ratio test was used to assess whether models significantly differed for each gene, with the test statistic calculated as two times the difference between the ln-likelihood of the branch model and the ln-likelihood of the null model, and *P*-values calculated from a c^2 approximation.¹³⁶

Characterizing the genomic landscape of divergence

To characterize the landscape of genomic divergence, we calculated genomic differentiation (F_{ST} , relative divergence) and divergence (d_{XY} , absolute divergence) between the sulfidic and nonsulfidic population of each species across non-overlapping 5-kb windows spanning the genome from our filtered dataset (excluding the two putative, early-stage hybrids in *Poecilia*, as described above) using the popgenWindows.py script.^{137–139} A 5-kb window size was selected because LD decays rapidly in all lineages investigated (Figure S7), and we were interested in detecting localized genomic divergences, but analyses with larger window sizes yielded similar results (not shown). Divergent selection between habitats should lead to elevated levels of both F_{ST} and d_{XY} at and around loci under selection (those contributing to the maintenance of adaptive divergence), while regions of the genome with reduced diversity in one or both populations (likely a consequence of background selection or low recombination rates) are expected to exhibit elevated F_{ST} but not d_{XY} .^{36,39,140} To identify probable targets of divergent selection between sulfidic and nonsulfidic populations, we used a composite outlier analysis of both statistics as implemented in the R package MINOTAUR.⁴⁰ First, we converted F_{ST} and d_{XY} to rank-based *P*-values using a right-tailed test, then $–\log_{10}$ -transformed these *P*-values, and calculated the Mahalanobis distances among windows (the “Md-rank-P” method recommended for summary statistics).⁴¹ We considered windows in the top 1% of the resulting Mahalanobis distance distribution as genomic regions likely experiencing divergent natural selection between habitat types in each species. We also identified regions that were classified as outlier windows across all three species and between each pairwise combination of species.

We investigated the link between divergent selection and the putative biological functions of genes found in these outlier windows for each species using a GO-enrichment analysis (as described above). We first identified genes in outlier regions from the *X. maculatus* genome annotation file (GTF) using the *intersect* tool in BEDTools v.2.25.0.¹¹³ We then annotated all genes that had a match in the human SWISSPROT database (21,891 genes) with GO IDs and tested for enrichment of specific GO IDs in outlier regions relative to all human annotated genes in the *X. maculatus* genome using GORILLA (*P*-value threshold: 0.0001, accessed 09/29/2020).¹⁰⁰ In total, 12,247 unique SWISSPROT annotations were associated with a GO term.

Scans for positive selection

To further test for signals of natural selection driving genomic divergence between sulfidic and nonsulfidic populations, we implemented the cross-population composite likelihood ratio (XP-CLR)⁴² test to identify regions of the genome with evidence for selective

sweeps in the sulfide spring population of each species based on differentiation in multilocus allele frequencies compared to the non-sulfidic population. We further filtered our biallelic SNP data to include only sites with no more than 10% missing data (957,379 in *Poecilia*, 2,885,156 in *Pseudoxiphophorus*, and 3,419,489 in *Xiphophorus*), and limited our analyses to chromosomes in the assembly, excluding all short scaffolds. For XP-CLR, the local two-dimensional site-frequency-spectrum (SFS) was compared to the genome-wide two-dimensional SFS to identify genomic regions putatively under selection.⁴² For each species, we designated the nonsulfidic population as the reference population, and the sulfidic population was the target population for each of the comparisons. Prior to running XP-CLR, we partitioned the genome into discrete 25-kb windows. If a window contained more than 200 SNPs, only the first 200 SNPs were used to calculate the composite likelihood ratio. The XP-CLR test statistic was not calculated if a window contained fewer than ten SNPs. We considered windows within the top 1% as putative selective sweeps.

Analysis of reciprocal translocation experiment

To analyze variation in survival, we used a generalized linear mixed model (GLMM) with a binomial error distribution and a logit-link function, as implemented in the R package LME4.⁹² Survival (binary data: 0 = died; 1 = survived) was used as the response variable. We included species, habitat of origin (sulfidic vs. nonsulfidic), and testing habitat (sulfidic vs. non-sulfidic) as fixed effects (including their interactions terms), and standard length (\log_{10} -transformed) as a covariate. Additionally, mesocosm ID was included as a random effect.